



1           **Clumped isotopes in near surface atmospheric CO<sub>2</sub> over land, coast and ocean in**  
2   **Taiwan and its vicinity**

3   Amzad H. Laskar<sup>1</sup> and Mao-Chang Liang<sup>1,2,3,4\*</sup>

4  
5           <sup>1</sup>Research Center for Environmental Changes, Academia Sinica, Taipei, Taiwan

6           <sup>2</sup>Graduate Institute of Astronomy, National Central University, Taiwan

7           <sup>3</sup>Institute of Astronomy and Astrophysics, Academia Sinica, Taiwan

8           <sup>4</sup>Department of Physics, University of Houston, USA

9

10       \*To whom correspondence should be addressed: [mcl@rcec.sinica.edu.tw](mailto:mcl@rcec.sinica.edu.tw)

11   Phone: (02) 2653-9885 #852

12   Fax:     (02) 2783-3584

13

14

15

16

17

18

19

20

21

22

23

24

25 **Abstract**

26 Molecules containing two rare isotopes (e.g.,  $^{13}\text{C}^{18}\text{O}^{16}\text{O}$  in  $\text{CO}_2$ ), called clumped isotopes, are  
27 powerful tools to provide an alternative way to independently constrain the sources of  $\text{CO}_2$  in  
28 the atmosphere because of their unique physical and chemical properties. We **present**  
29 clumped isotope data ( $\Delta_{47}$ ) in near surface atmospheric  $\text{CO}_2$  from urban, sub-urban, ocean,  
30 coast, high mountain (~3.3 km a.s.l.) and forest in Taiwan and its vicinity. The primary goal  
31 of the study **is** to use the unique  $\Delta_{47}$  signature in air  $\text{CO}_2$  to show the extents of its deviations  
32 from thermodynamic equilibrium due to different processes in a variety of environments,  
33 **which** the commonly used tracers such as  $\delta^{13}\text{C}$  and  $\delta^{18}\text{O}$  cannot provide. We also **explore** the  
34 **potential** of  $\Delta_{47}$  in air  $\text{CO}_2$  to identify/quantify the contribution from various sources.  
35 Atmospheric  $\text{CO}_2$  over ocean **is** found to be in thermodynamic equilibrium with the  
36 surrounding surface sea water. **Also** respired  $\text{CO}_2$  **is** in close thermodynamic equilibrium at  
37 ambient air temperature. In contrast, photosynthetic activity results in significant deviation in  
38  $\Delta_{47}$  values from that expected thermodynamically ~~demonstrated using  $\text{CO}_2$  collected from a~~  
39 ~~controlled greenhouse~~. The disequilibrium could be a consequence of kinetic effects  
40 associated with the diffusion of  $\text{CO}_2$  in and out of the leaf stomata. We also **observe** that  $\delta^{18}\text{O}$   
41 and  $\Delta_{47}$  behave differently in response to photosynthesis unlike simple water- $\text{CO}_2$  exchange  
42 where the time scale of equilibration of the two is similar. **Additionally**, the measured  $\Delta_{47}$   
43 values in car exhaust  $\text{CO}_2$  **are** significantly lower than the atmospheric  $\text{CO}_2$  but higher than  
44 that expected at the combustion temperature. In urban and sub-urban regions, the  $\Delta_{47}$  values  
45 **are** found to be lower than the thermodynamic equilibrium values at the ambient temperature,  
46 suggesting contributions from local combustion emissions.

47

48

49

50

51

52 **Keywords:** clumped isotopes; atmospheric  $\text{CO}_2$ ; thermodynamic equilibrium; anthropogenic;

53 car exhaust

54 **1. Introduction**

55 The budget of atmospheric CO<sub>2</sub> is widely studied using the temporal and spatial variations of  
 56 ~~the~~ <sup>in</sup> concentration and bulk isotopic compositions ( $\delta^{13}\text{C}$  and  $\delta^{18}\text{O}$ ) of CO<sub>2</sub> (Francey and Tans,  
 57 1987; Francey et al., 1995; Yakir and Wang, 1996; Ciais et al., 1995a,b, 1997; Peylin et al.,  
 58 1999; Cuntz et al., 2003; Drake et al., 2011; Welp et al., 2011; Affek and Yakir., 2014).  $\delta^{13}\text{C}$   
 59 is useful to differentiate the exchange of CO<sub>2</sub> with the ocean and land biospheres as the  
 60 photosynthetic discrimination against  $^{13}\text{C}$  during exchange with land plants is higher than that  
 61 associated with the chemical dissolution of CO<sub>2</sub> in the ocean (e.g., Tans et al., 1993; Ciais et  
 62 al., 1995a; Francey et al., 1995; Ito, 2003; Bowling et al., 2014).  $\delta^{18}\text{O}$  is used for partitioning  
 63 global-scale net CO<sub>2</sub> terrestrial fluxes between photosynthesis and respiration (Francey and  
 64 Tans, 1987; Farquhar and Lloyd, 1993; Yakir and Wang, 1996; Ciais et al., 1997; Peylin et  
 65 al., 1999; Murayama et al., 2010; Welp et al., 2011). ~~This is because oxygen isotopes in CO<sub>2</sub>,  
 66 exchanges readily with water and hence the values of  $\delta^{18}\text{O}$  are different when exchanging  
 67 with soil water or relatively enriched leaf water; the enrichment in  $^{18}\text{O}$  in the leaf water  
 68 occurs during evapotranspiration.~~ The major limitation of  $\delta^{13}\text{C}$  is that it cannot distinguish  
 69 between CO<sub>2</sub> produced from high temperature combustion and low temperature respiration.  
 70  $\delta^{18}\text{O}$  in atmospheric CO<sub>2</sub> is mainly controlled by various water reservoirs (ocean, leaf, and  
 71 soil). In urban locations, a significant fraction of CO<sub>2</sub> may have combustion origin possessing  
 72  $\delta^{18}\text{O}$  signature of atmospheric O<sub>2</sub> (Kroopnick and Craig, 1972; Ciais et al., 1997; Yakir and  
 73 Wang, 1996; Barkan and Luz, 2012). The  $\delta^{18}\text{O}$  values from these processes and interactions  
 74 are different. ~~As a result,~~  $\delta^{18}\text{O}$  in atmospheric CO<sub>2</sub> has been widely used for constraining the  
 75 budget of CO<sub>2</sub> (Francey and Tans, 1987; Ciais et al., 1997; Gillon and Yakir, 2001; Cuntz et  
 76 al., 2003; Welp et al., 2011). However, due to ~~its~~ short turnover time in the atmosphere,  
 77 mainly ~~affected by presence~~ of enzyme carbonic anhydrase in plants, soils, and surface ocean,  
 78 the definite determination of the associated fluxes in CO<sub>2</sub> biogeochemical models remains  
 79 inconclusive. <sup>Furthermore,</sup> The presence of diverse  $\delta^{18}\text{O}$  reservoirs and processes such as  
 80 evapotranspiration ~~also~~ complicates the interpretation.

81

82 The doubly substituted isotopologues or clumped isotopes such as  $^{13}\text{C}^{18}\text{O}^{16}\text{O}$  in CO<sub>2</sub>, whose  
 83 excess over the stochastic isotopic distribution, denoted by  $\Delta_{47}$ , provides an additional and  
 84 independent constraint to study the atmospheric CO<sub>2</sub> budget and mechanisms for CO<sub>2</sub>  
 85 production and consumption. Unlike bulk isotopes, clumped isotope studies for the



86 atmospheric CO<sub>2</sub> are very limited mainly because of the challenges to acquire it precisely  
87 (Eiler and Schauble, 2004; Affek et al., 2007; Yeung et al., 2009). The available data are not  
88 sufficient to address some key issues such as quantification of CO<sub>2</sub> from different sources and  
89 to what extent the air CO<sub>2</sub> is in thermodynamic equilibrium with leaf and surface waters,  
90 especially in regions with strong anthropogenic activities such as urban areas. Also the effect  
91 of photosynthesis on the  $\Delta_{47}$  of air CO<sub>2</sub> has not been studied rigorously.  $\delta^{18}\text{O}$  and  $\Delta_{47}$  were  
92 reported to have similar isotope exchange time scales with pure water (Affek, 2013; Clog et  
93 al., 2015), but how they behave in presence of other processes such as photosynthesis and  
94 respiration has not been studied well. A combined assessment from all of the three  
95 aforementioned isotopic tracers can better constrain the budget of CO<sub>2</sub> and associated  
96 processes than  $\delta^{13}\text{C}$  or  $\delta^{18}\text{O}$  alone.

97

98 Theoretically it is shown that in thermodynamic equilibrium,  $\Delta_{47}$  values of CO<sub>2</sub> are  
99 temperature dependent (Eiler and Schauble, 2004; Wang et al., 2004), verified over a wide  
100 range from 10 to 1000 °C (Dennis et al., 2011). Processes that involve CO<sub>2</sub> and liquid water  
101 as medium, such as isotopic exchange with ocean water are expected to have  $\Delta_{47}$  values close  
102 to the thermodynamic equilibrium.  $\Delta_{47}$  values in ambient air CO<sub>2</sub> should reflect a balance of  
103 CO<sub>2</sub> fluxes between biosphere-atmosphere exchange, ocean-atmosphere exchange, and  
104 emissions from combustion sources. Photosynthesis involves gas phase diffusion of CO<sub>2</sub> into  
105 leaves, fixes ~1/3 of the CO<sub>2</sub>, and returns the rest back to the atmosphere. CO<sub>2</sub> molecules  
106 inside a leaf are generally expected to be in thermodynamic equilibrium with leaf water  
107 because of presence of enzymatic carbonic anhydrase that greatly enhances the isotopic  
108 exchange (Cernusak et al., 2004).  $\Delta_{47}$  values of soil respired CO<sub>2</sub> is also not well constrained,  
109 though it is believed to be in thermodynamic equilibrium with the soil water.

110 Here, we present clumped and bulk isotope data in near surface air CO<sub>2</sub> covering a wide  
111 variety of processes and interactions. Air samplings were made in South China Sea, two  
112 coastal stations in northern Taiwan, an urban traffic street, a sub-urban location, a forest site,  
113 a greenhouse, top of a high mountain, and car exhausts. The study is designed and aimed to  
114 show the extents of the deviations of near surface atmospheric CO<sub>2</sub> from thermodynamic  
115 equilibrium with local surface water. Possible influences from other processes such as  
116 anthropogenic emission, respiration, and photosynthesis on clumped isotopes are explored.  
117 We show that CO<sub>2</sub> respired from root and soil is in close thermodynamic equilibrium with the



118 soil waters but photosynthesis tends to deviate it. Therefore, utilizing  $\Delta_{47}$  for partitioning  
119 fluxes between photosynthesis and respiration/soil invasion is possible.

120

121

## 122 **2. Materials and methods**

123 Stable isotopic compositions of  $\text{CO}_2$  including mass 47 amu were measured using a Finnigan  
124 MAT 253 gas source stable isotope ratio mass spectrometer configured to measure ion beams  
125 corresponding to M/Z 44 through 49. The instrument registers the major ion beams (44, 45  
126 and 46) through resistors  $10^8$ ,  $3 \times 10^{10}$ , and  $10^{11}$  Ohm, respectively, and minor ion beams (47,  
127 48 and 49) through  $10^{12}$  Ohm. All the measurements were carried out at Research Center for  
128 Environmental Changes, Academia Sinica, Taiwan.

129

130 Air samples were collected in 2L flasks and compressed to 2 atmosphere pressure using a  
131 membrane pump; the flasks were first flushed with the ambient air for ~10 min before sample  
132 collection. The air was pumped through a column packed with magnesium perchlorates to  
133 remove moisture. The moisture content was reduced from the ambient value of 70-90 % to  
134 less than 1 % relative humidity, checked using a LI-COR infrared gas analyzer (model 840A,  
135 LI-COR, USA).

136

137 To show how photosynthesis and respiration affect the abundances of  $\text{CO}_2$  isotopologues and  
138 to demonstrate what different information the  $\Delta_{47}$  can give from the other isotopologues, we  
139 performed systematic analyses for  $\text{CO}_2$  collected in a controlled greenhouse with cemented  
140 floor located in the top (3<sup>rd</sup>) floor of the Greenhouse Building, Academia Sinica. The size of  
141 the greenhouse was about 8m long, 5m wide and 5m high, and was in a condition to have  
142 minimal air exchange with the surroundings by switching off the ventilation system. More  
143 than 70 % of the ground area inside the greenhouse was occupied with *Cinnamomum cassia*  
144 plants, each of ~2 m height kept in pots. Samples were collected at intervals of less than half  
145 an hour to a few hours on three sunny days and one cloudy day to investigate the influence of  
146 photosynthesis and respiration on the isotopologues of  $\text{CO}_2$ . The greenhouse was isolated  
147 from the surroundings at least a day before the sample collection; the room relative humidity  
148 was ~50-70 % for the three sunny days and was above 90 % for the cloudy day.

149



150 Forest air CO<sub>2</sub> was collected from a dense natural forest at the west end of the Academia  
151 Sinica Campus. The samples were collected ~100 m inside the forest on a small plateau at a  
152 height of ~30 m from the ground in the slope of a hill; the dense vegetation allowed little  
153 sunlight penetrating to the surface. The relative humidity at the site was 80-90 % during the  
154 sampling days and wind speed was nearly zero due to presence of hills on three sides of the  
155 sampling spot. Marine air was collected during a cruise in the South China Sea (for the cruise  
156 track see Figure 1) and from two coastal stations: Keelung (25°09'6" N, 121°46'22" E) and  
157 Fuguei Cape (25°18' N, 121°32' E) (Figure 1). Urban air was collected at a bus stop on  
158 Roosevelt Road, a busy street in Taipei. Sub-urban air was collected from an open roof (~30  
159 m above ground) of Institute of Earth Science Building, Academia Sinica (AS; 25°2'41" N,  
160 121°36'52" E); grassland air was collected from a grass field in front of the Department of  
161 Atmospheric Science, National Taiwan University Campus (NTU; 25° 1' N, 121°30' E),  
162 Taipei. In addition, we collected air from the summit of the Hehuan mountain (24°8'15" N,  
163 121°16'32" E, 3.3 km a.s.l.) (Figure 1) on 9<sup>th</sup> October, 2013. All air samplings were made  
164 when there was no rain to avoid direct interaction with the rainwater. Car exhausts were  
165 collected from a Mazda 3000cc TRIBUTE and a Mitsubishi 2400cc New Outlander, using  
166 evacuated 2L glass flasks from ~20 cm inside the exhaust pipes through a column of  
167 magnesium perchlorate.

168

169 CO<sub>2</sub> was extracted from air by cryogenic technique. Air in the flask was pumped through a  
170 series of five coiled traps, with the first two immersed in dry ice-ethyl alcohol slush (-77 °C)  
171 for trace moisture removal followed by three in liquid nitrogen (-196 °C). CO<sub>2</sub> was collected  
172 from the traps immersed in liquid nitrogen by repeated freeze-thaw technique at liquid  
173 nitrogen and dry ice temperatures for further removal of traces of water [see Mahata *et al.*,  
174 2012 for details]. The air was pumped for 40-45 minutes at a controlled rate of ~90 mL/min  
175 using a mass flow controller; the pressure on the post mass flow controller was ~10 mm of  
176 Hg. No measurable isotopic fractionation caused by mass flow controller at this flow rate was  
177 observed, checked using several aliquots of air from a high volume compressed air cylinder  
178 (~40 L at 2000 psi). For car exhaust, an aliquot of exhaust air was transferred to a 60 mL



179 bottle and CO<sub>2</sub> was fully extracted cryogenically following the same protocol as discussed  
180 above (but with mass flow controller step skipped).

181

182 CO<sub>2</sub> was further purified from other condensable species like N<sub>2</sub>O, CH<sub>4</sub>, and hydrocarbons  
183 by means of gas chromatography (Agilent 6890N, with a 3.0 m × 0.3 cm stainless steel  
184 column packed with PorapakQ 80/100 mesh, supplied by Supelco Analytical, Bellefonte, PA,  
185 USA) with the column kept at -10 °C. High purity helium (>99.9999 % supplied by Air  
186 Products and Chemicals, Inc.) at 20 mL/min was used as carrier gas. CO<sub>2</sub> was eluted first,  
187 followed forthwith by N<sub>2</sub>O, and CH<sub>4</sub>, hydrocarbons and traces of water came out much later.  
188 To get an optimized condition for CO<sub>2</sub>, we checked the separation of CO<sub>2</sub> from N<sub>2</sub>O with  
189 varying proportions and at various temperatures (25 °C to -20 °C) and found a temperature of  
190 -10 °C at which column separated CO<sub>2</sub> from N<sub>2</sub>O perfectly (see Supporting Information). The  
191 column was baked at 200 °C for more than 2 hours prior to use. The conditioned column is  
192 good for purifying three samples. At the end of the day, long baking (8-10 hours) was  
193 performed. At the initial phase the working gas was taken from a high purity commercial CO<sub>2</sub>  
194 called AS-2 (δ<sup>13</sup>C = -32.54 ‰ and δ<sup>18</sup>O = 36.61 ‰) procured from a local supplier (Air  
195 Products and Chemicals, Inc.). As the difference between the isotopic compositions of  
196 samples and AS-2 was high, we later changed the reference to Oztech CO<sub>2</sub> (δ<sup>13</sup>C = -3.59‰  
197 and δ<sup>18</sup>O = 24.96 ‰) (Oztech Trading Corporation, USA) from December 2014 onward. No  
198 detectable difference in isotopic compositions including Δ<sub>47</sub> was observed between the  
199 analyses from different working references. All δ<sup>13</sup>C values are expressed in VPDB scale and  
200 δ<sup>18</sup>O in VSMOW scale, unless specified otherwise. Δ<sub>47</sub> is calculated following (Affek and  
201 Eiler, 2006):

$$202 \quad \Delta_{47} = \left[ \frac{R^{47}}{2R^{13}R^{18} + 2R^{17}R^{18} + R^{13}(R^{17})^2} - \frac{R^{46}}{2R^{18} + 2R^{13}R^{17} + (R^{17})^2} - \frac{R^{45}}{R^{13} + 2R^{17}} + 1 \right] \times 1000 \quad (1)$$

203 where  $R^{13}$  and  $R^{18}$  (ratios <sup>13</sup>C/<sup>12</sup>C and <sup>18</sup>O/<sup>16</sup>O) are obtained by measuring the traditional  
204 masses 44, 45 and 46 in the same CO<sub>2</sub> sample and  $R^{17}$  is calculated assuming a mass  
205 dependent relation with  $R^{18}$  given by  $R^{17} = R^{17}_{VSMOW} \left( \frac{R^{18}}{R^{18}_{VSMOW}} \right)^\lambda$ , where exponent  
206  $\lambda = 0.5164$  is used for all Δ<sub>47</sub> calculations (Affek and Eiler, 2006). The value of  $\lambda$  varies  
207 between 0.516 and 0.523 (Hoag et al., 2005; Barkan and Luz, 2012; Hoffmann et al., 2012;  
208 Thiemens et al., 2014). The variation in Δ<sub>47</sub> is less than 0.01 ‰ at 25 °C when the exponent is  
209 varied over the aforementioned range. This variation is comparable to the measurement



210 uncertainty and hence is not considered here; all the calculations are based on  $\lambda=0.5164$ .  $\Delta_{47}$   
211 is obtained by measuring  $\text{CO}_2$  with respect to which the isotopes among various  $\text{CO}_2$   
212 isotopologues are distributed randomly ( $\Delta_{47} \sim 0$  ‰). Practically, this limit is approached by  
213 heating  $\text{CO}_2$  at 1000 °C for more than two hours (Eiler and Schauble, 2004; Affek and Eiler,  
214 2006). Measurements were made with a stable ~12 volt signal at mass 44, with peak centring,  
215 background scanning, and pressure-balancing before each acquisition started. Each sample  
216 was analyzed for 10 acquisitions, 10 cycles each at an integration time of 8 s; the total  
217 analysis time was approximately 2.5 h. Routine analysis of masses 48 and 49, in addition to  
218 masses 44 to 47 was used to monitor the degree of possible interference of sample impurities  
219 on the measurements of  $\Delta_{47}$  (Ghosh et al., 2006).

220

221 Dependence of  $\Delta_{47}$  on  $\delta^{47}$  was derived by artificially varying the  $\delta^{47}$  value by ~130 ‰ (Figure  
222 S1 in Supporting Information).  ~~$\delta^{47}$  is approximately~~ equal to the sum of  $\delta^{13}\text{C}$  and  $\delta^{18}\text{O}$   
223 measured with respect to the working gas. The wide range in  $\delta^{47}$  was obtained by  
224 equilibrating AS-2  $\text{CO}_2$  with different waters covering a wide range of  $\delta^{18}\text{O}$  (-106 to +22 ‰)  
225 at two temperatures (17 and 32 °C).  $\text{CO}_2$  was separated from water- $\text{CO}_2$  mixture  
226 cryogenically and purified using gas chromatography as mentioned earlier. The extracted  
227  $\text{CO}_2$  was divided into two aliquots: one was directly analyzed in the mass spectrometer and  
228 the other was measured after heating at 1000 °C (to define scrambled/stochastic distribution)  
229 for more than two hours. A weak dependence of  $\Delta_{47}$  on  $\delta^{47}$  with a slope of -0.0017‰/‰  
230 ( $\Delta_{47}/\delta^{47}$ ) was observed. No pressure baseline correction was made considering the little  
231 dependence of  $\Delta_{47}$  on  $\delta^{47}$  (He et al., 2012). The calibration curve was then applied evenly to  
232 all samples to remove the dependence of  $\Delta_{47}$  on  $\delta^{47}$  (Ghosh et al., 2006; Huntington et al.,  
233 2009; Dennis et al., 2011). Details are provided in the Supporting Information.

234

235 The reference frame equation or empirical transfer function can then be derived from these  
236 three temperature experiments. All the  $\Delta_{47}$  values are expressed in absolute reference frame  
237 (ARF) (Dennis et al., 2011). The empirical transfer function for the present case is  
238  $\Delta_{47-RF} = 1.0996 \Delta_{47-[EGvsWG]_0} + 0.9145$  with  $R^2 = 0.9999$  ( $n=3$ ), where  $\Delta_{47-RF}$  is the  $\Delta_{47}$  value in  
239 the ARF and  $\Delta_{47-[EGvsWG]_0}$  is the intercept of the  $\Delta_{47}$  versus  $\delta^{47}$  plot. To obtain the temperature  
240 from the  $\Delta_{47}$  values, we used the following relation (Dennis et al., 2011):





$$\Delta_{47} = 0.003 \left( \frac{1000}{T} \right)^4 - 0.0438 \left( \frac{1000}{T} \right)^3 + 0.2553 \left( \frac{1000}{T} \right)^2 - 0.2195 \left( \frac{1000}{T} \right) + 0.0616 \quad (2)$$

242

243 The reproducibility (1- $\sigma$  standard deviation) for air CO<sub>2</sub> measurements was established from  
244 three aliquots of CO<sub>2</sub> extracted from a compressed air cylinder with CO<sub>2</sub> concentration  
245 ([CO<sub>2</sub>]) of ~388 ppmv. The 1- $\sigma$  standard deviations were 0.07, 0.08, and 0.01 ‰ for  $\delta^{13}\text{C}$ ,  
246  $\delta^{18}\text{O}$ , and  $\Delta_{47}$ , respectively (Table S1). We also used IAEA NBS-19 carbonate standard to  
247 check the reproducibility of our measurements routinely. For carbonate analysis, CO<sub>2</sub> was  
248 produced by reacting with ~104 % orthophosphoric acid at 25 °C. The measured isotopic data  
249 including  $\Delta_{47}$  for NBS-19 are presented in Table 1, and the long term reproducibility is 0.014  
250 ‰ (1- $\sigma$  standard deviation; n=15). The accuracy from the measurements of NBS-19 is  
251 difficult to check, due to poor consensus of the reported  $\Delta_{47}$  values from different  
252 laboratories; our values fall within the range. To further verify the accuracy, we equilibrated  
253 cylinder CO<sub>2</sub> (AS-2) with water at 15±2 °C and 25±2 °C, chosen to represent the ambient  
254 temperatures presented in the current study. The deviation of temperature from the expected  
255 values obtained from  $\Delta_{47}$  was found to vary between -1 to +3 °C (Table S2).

256 For [CO<sub>2</sub>] measurements, flasks of volume 350 cc were used. These small flasks were  
257 connected in series with the larger flasks used for isotopic measurements. [CO<sub>2</sub>] was  
258 measured using a LI-COR infrared gas analyzer (model 840A, LI-COR, USA) at 4 Hz,  
259 smoothed with 20-s moving average. The analyzer was calibrated against a working standard  
260 (air compressed in a cylinder) with a nominal [CO<sub>2</sub>] of 387.7 ppmv and a CO<sub>2</sub> free N<sub>2</sub>  
261 cylinder. The reproducibility of LI-COR is better than 1 ppmv. The working standard was  
262 calibrated using a commercial Picarro analyzer (model G1301, Picarro, USA) by a series of  
263 NOAA/GMD certified tertiary standards with [CO<sub>2</sub>] of 369.9, 392.0, 409.2, and 516.3 ppmv,  
264 with a precision (1- $\sigma$  standard deviation) of 0.2 ppmv. The [CO<sub>2</sub>] in car exhausts were  
265 estimated by gravimetric technique using an MKS Baratron gauge.

266

267 Ambient temperatures were taken from the nearest governmental weather stations (operated  
268 by Central Weather Bureau, Taiwan): Nankang (for AS; station code: C0A9G0; 25°03'27"

269 N, 121°35'41" E, 42 m a.s.l.), Taipei (for NTU; station code: C1A730; 25°00' 58" N,

270 121°31' 53" E; 22 m a.s.l.), Hehuan mountain (station code: C0H9C1; 24°08'41" N, 121°15'




271 51" E, 3240 m a.s.l.), and Keelung coast (for the two coastal sites; station code: 466940;



272 25°08'05" N, 121°43'56" E, 26.7 m a.s.l.). 

273


### 274 3. Results

#### 275 3.1 Greenhouse CO<sub>2</sub>

276 Intraday variation in the concentration and isotopic compositions of CO<sub>2</sub> inside the controlled  
277 greenhouse is shown in Figure 2. The lowest  [CO<sub>2</sub>] and highest δ<sup>13</sup>C and δ<sup>18</sup>O values are  
278 observed during late morning hours while highest [CO<sub>2</sub>] and lowest δ<sup>13</sup>C and δ<sup>18</sup>O values are  
279 observed during night time and early morning before sunrise (Table 2 and Figure 2A-2C),  
280 indicating that respiration and photosynthesis play the major role in controlling the variations  
281 of the [CO<sub>2</sub>] and isotopic compositions. Keeling graphical analysis for δ<sup>13</sup>C gives an intercept  
282 of -26.32±0.40 ‰ (Figure 2D), a value expected for C<sub>3</sub> plant respired CO<sub>2</sub>. The Keeling plot  
283 for δ<sup>18</sup>O gives an intercept of 30.68±0.73 ‰ (Figure 2E), which could be explained by a  
284 combined effect of respired CO<sub>2</sub> equilibrated with soil water and kinetic fractionation  
285 associated with the diffusion of CO<sub>2</sub> from soil to the air. The tight correlations among [CO<sub>2</sub>],  
286 δ<sup>13</sup>C and δ<sup>18</sup>O (Figure 2D-2F), however, suggest that photosynthesis/respiration are the  
287 dominant processes controlling their variations ~~and the~~ mixing with ambient air and  
288 anthropogenic contribution of CO<sub>2</sub> are insignificant.

289 In contrast, Δ<sub>47</sub> shows different patterns of diurnal variability. Figures 3A-3D detail diurnal  
290 variations in Δ<sub>47</sub> in the greenhouse CO<sub>2</sub> in four different days. The first three are bright sunny  
291 days while the last one is a dark cloudy day; to further reduce photosynthetic activity, two  
292 layers of black cloths that cut down incident sunlight by ~50% are deployed for the last. The  
293 measured Δ<sub>47</sub> values are also compared with the thermodynamic equilibrium. The maximum  
294 value of Δ<sub>47</sub> is observed in the morning before ~8 AM and at night: the values are similar to  
295 that expected at the ambient temperatures, indicating that the respired CO<sub>2</sub> is in close  
296 thermodynamic  equilibrium. The daytime Δ<sub>47</sub> values are, in general, higher than the  
297 thermodynamic equilibrium values. By comparing the Δ<sub>47</sub> values acquired in the sunny days  
298 with that in the cloudy day, we notice that when photosynthesis is weak, the Δ<sub>47</sub> value is close  
299 to the thermodynamic equilibrium (Figure 4). No correlation (R<sup>2</sup> < 0.1) is observed between  
300 Δ<sub>47</sub> and [CO<sub>2</sub>], δ<sup>13</sup>C or δ<sup>18</sup>O (Figure 3A-C)  when the photosynthesis is weak (Figure



301 3D), which suggests that the  $\Delta_{47}$  carries information different from concentration and bulk  
302 isotopes when photosynt  occurs. See Section 4.1 for detailed discussion.

303

### 304 3.2 Car exhaust

305 The concentration,  $\delta^{13}\text{C}$  and  $\delta^{18}\text{O}$  values of car exhaust  $\text{CO}_2$  are  $39350 \pm 50$  ppmv, -  
306  $27.70 \pm 0.03$  ‰ and  $25.35 \pm 0.07$  ‰, respectively (Table 3).  $\delta^{13}\text{C}$  value is similar to that  
307 reported elsewhere (Newman et al., 2008; Popa et al., 2014), the  $\delta^{18}\text{O}$  is slightly higher than  
308 the atmospheric  $\text{O}_2$  ( $\sim 23.5$  ‰), the source of  $\text{O}_2$  for combustion. This is probably due to post  
309 isotopic exchange with water present in the stream of the exhaust inside the catalytic  
310 converter and the exhaust pipe. The average value of  $\Delta_{47}$  for the exhausts from the two cars is  
311  $0.273 \pm 0.021$  ‰, which gives an average temperature of  $282 \pm 17$  °C (Table 3).

312

### 313 3.3 $\text{CO}_2$ over ocean, coasts and land

314 Isotopic compositions including  $\Delta_{47}$  values obtained for  $\text{CO}_2$  over ocean, coasts, sub-urban,  
315 and grassland are summarized in Table 4 and 5. The averaged  $[\text{CO}_2]$  over ocean between  
316 latitudes  $18^\circ 03'$  N and  $21^\circ 17'$  N is  $395 \pm 7$  ppmv, and the values of  $\delta^{13}\text{C}$  and  $\delta^{18}\text{O}$  are -  
317  $8.43 \pm 0.19$  ‰ and  $40.72 \pm 0.20$  ‰, respectively (Table 4). Figure 5 shows a comparison of  
318 carbon Keeling analyses for the atmospheric  $\text{CO}_2$  collected over different regions. The  
319 intercept for oceanic  $\text{CO}_2$  is  $-15.96 \pm 1.95$  ‰ (Figure 5A). In the coastal stations, the averaged  
320 values of  $[\text{CO}_2]$ ,  $\delta^{13}\text{C}$ , and  $\delta^{18}\text{O}$  are  $397 \pm 10$  ppmv,  $-8.48 \pm 0.11$  ‰, and  $40.70 \pm 0.29$  ‰,  
321 respectively, with a  $\delta^{13}\text{C}$  Keeling intercept of  $-12.20 \pm 1.11$  ‰ (Figure 5B). Both the  $[\text{CO}_2]$   
322 and  $\delta^{13}\text{C}$  values over the ocean and coasts are similar to those observed at Mauna Loa during  
323 the sampling period, suggesting little contribution from local/regional anthropogenic sources.  
324 However, the intercepts of the Keeling plots is different from the  $\delta^{13}\text{C}$  value of the  $\text{CO}_2$   
325 released by the remineralization of organic matter ( $-20$  to  $-30$  ‰) in the deep sea regions, the  
326 expected source of  $\text{CO}_2$  over ocean. This is probably due to partial isotopic equilibration of  
327 the  $\text{CO}_2$  with dissolved inorganic carbon before releasing to the atmosphere (see discussion  
328 for details).

329



330 The averaged values of  $[\text{CO}_2]$ ,  $\delta^{13}\text{C}$ , and  $\delta^{18}\text{O}$  for air  $\text{CO}_2$  near Roosevelt Road, a busy street  
331 in downtown Taipei, are  $500\pm 50$  ppmv,  $-11.05\pm 0.90$  ‰, and  $39.319\pm 0.94$  ‰, respectively  
332 (Table 5). Both the  $[\text{CO}_2]$  and isotopic compositions show signatures of a significant  
333 contribution from vehicular emissions. In the sub-urban location (AS),  $[\text{CO}_2]$  averaged over  
334 four months is  $410\pm 10$  ppmv (Table 5),  $\sim 15$  ppmv higher than that observed over the South  
335 China Sea and that at Mauna Loa Observatory during the time of sampling. The higher  $[\text{CO}_2]$   
336 suggests contribution from local anthropogenic emissions.  $\delta^{13}\text{C}$  values mainly vary between -  
337 7.83 to  $-10.30$  ‰, with an average of  $-8.78\pm 0.50$  ‰. Keeling analysis for  $\delta^{13}\text{C}$  (Figure 5C)  
338 gives an intercept of  $-26.16\pm 1.58$  ‰, indicating source of  $\text{CO}_2$  from  $\text{C}_3$  plant respiration  
339 and/or combustion. The averaged  $[\text{CO}_2]$  over the grassland (NTU) is  $410\pm 33$  ppmv. The  
340 Keeling plot intercept is  $-16.98\pm 1.02$  ‰ (Figure 5D), indicating a significant fraction of  $\text{CO}_2$   
341 originated from  $\text{C}_4$  vegetation. This is not surprising as the  $\text{CO}_2$  was sampled over a  $\text{C}_4$   
342 dominated grassland (area:  $\sim 50$  m x 50 m). We note that though the station is located in an  
343 urban region, the sampling location is at least  $\sim 150$  m away from traffic streets, such as  
344 Keelung road, along with  $\sim 60$  m wide,  $\sim 10$  m high  $\text{C}_3$  trees in between. As a result,  
345 anthropogenic signals are not very prominent. The averaged values of  $\delta^{13}\text{C}$  and  $\delta^{18}\text{O}$  are -  
346  $8.95\pm 0.70$  ‰ and  $39.74\pm 1.00$  ‰, respectively. Unlike greenhouse  $\text{CO}_2$ , no statistically  
347 significant correlation between  $\delta^{18}\text{O}$  and  $1/[\text{CO}_2]$  in air  $\text{CO}_2$  in these sites is observed (not  
348 shown), probably due to various contributions from multiple sources and processes affecting  
349  $\text{CO}_2$ .

350 The  $[\text{CO}_2]$ ,  $\delta^{13}\text{C}$ , and  $\delta^{18}\text{O}$  values for two high mountain air  $\text{CO}_2$  samples collected on 9<sup>th</sup>  
351 October, 2013 are 364 ppmv,  $-8.23\pm 0.02$  ‰ and  $40.59\pm 0.30$  ‰, respectively (Table 5). The  
352 lower  $[\text{CO}_2]$  and higher  $\delta^{13}\text{C}$  than Mauna Loa suggests photosynthetic uptake, which is also  
353 seen at NTU site and inside greenhouse on a few occasions. The air  $[\text{CO}_2]$ ,  $\delta^{13}\text{C}$  and  $\delta^{18}\text{O}$  are  
354  $438\pm 16$  ppmv,  $-9.99\pm 0.50$  ‰ and  $40.39\pm 0.63$  ‰, respectively, for a dense forest site near the  
355 Academia Sinica (AS) Campus. Given the proximity of the site from AS, the higher  
356 concentration and lower  $\delta^{13}\text{C}$  values than those at AS indicate significant influence from local  
357 respiration (Table 5).

358 Figure 6 shows the time series of  $\delta^{13}\text{C}$  and  $\delta^{18}\text{O}$  at the sub-urban station where measurements  
359 were carried out for more than four months. Tentatively,  $[\text{CO}_2]$  level increases and  $\delta^{13}\text{C}$   
360 depletes from October to February (Figure 6A), likely a result of seasonal variation in  
361 photosynthesis/respiration. On average, the  $\delta^{13}\text{C}$  value is slightly less than the global mean,



362 implying influence from local/regional anthropogenic activities though the dominant role is  
363 played by biogeochemistry in affecting the variation. The time series of  $\delta^{18}\text{O}$  (Figure 6B)  
364 shows variation between 39.40 and 41.57 ‰, with an average of  $40.87 \pm 0.46$  ‰. An  
365 increasing trend is also observed in  $\delta^{18}\text{O}$  from October to February. We attribute this to  
366 interactions with rain and surface waters which are heavier in winter time compared to the  
367 summer (Peng et al., 2010; Laskar et al., 2014).


368 The  $\Delta_{47}$  values vary between 0.880 ‰ to 0.946 ‰ for the marine and coastal  $\text{CO}_2$  (Table 4,  
369 Figures 7A and 7B), similar to that predicted at thermodynamic equilibrium at sea surface  
370 temperatures (obtained using equation (2)). Similarly,  $\delta^{18}\text{O}$  of air  $\text{CO}_2$  shows the expected  
371 equilibrium values with the surface sea water (see discussion), suggesting that the air  $\text{CO}_2$  is  
372 indeed in thermodynamic equilibrium with the underlying sea water. Figure 7C shows the  
373 measured  $\Delta_{47}$  values at the sub-urban station along with the equilibrium values expected at  
374 the ambient temperatures. Here the  $\Delta_{47}$  values vary between 0.853 ‰ and 0.972 ‰, which in  
375 contrast to the marine  $\text{CO}_2$ , are significantly less than the thermodynamic equilibrium values  
376 (assuming water bodies have the same temperature as the ambient) (Table 5). Figure 7D  
377 shows the  $\Delta_{47}$  values in the grassland (NTU). A large variation in  $\Delta_{47}$  is observed (0.885 -  
378 0.989 ‰) with an average of  $0.937 \pm 0.030$  ‰; some of the values are close to the  
379 thermodynamic equilibrium while the others deviated significantly. The forest air  $\text{CO}_2$   $\Delta_{47}$   
380 values in summer fall in the range of 0.887 ‰ to 0.920 ‰, with an average of  $0.895 \pm 0.012$   
381 ‰ (Table 5). The values are similar to that at thermodynamic equilibrium (Figure 7E) except  
382 on 11<sup>th</sup> August, when a significant increase in  $\Delta_{47}$  was observed. The deviation is probably  
383 due to influence of a super typhoon, which passed over the region on previous days mixing  
384 and transporting air masses regionally. In the high mountain station, the averaged value of  
385  $\Delta_{47}$  is  $0.904 \pm 0.009$  ‰, slightly less than that expected at the ambient temperature (Table 5).


386 To show how anthropogenic emission affects the background  $\Delta_{47}$  values, we collected several  
387 air  $\text{CO}_2$  samples from Roosevelt Road and the values are in the range of 0.754‰ to 0.833 ‰,  
388 with an average of  $0.807 \pm 0.028$  ‰ (Figure 7F). The value is lower by  $\sim 0.16$  ‰ compared to  
389 the thermodynamic equilibrium value, indicating a significant fraction of  $\text{CO}_2$  produced at  
390 higher temperatures.


391

#### 392 4. Discussion



393 As stated earlier, the  $\Delta_{47}$  has the unique physical property of representing the formation  
394 temperature of a  $\text{CO}_2$  molecule, providing an alternative tool for constraining the budget of  
395  $\text{CO}_2$  in the atmosphere. We present in detail the data of multiple  $\text{CO}_2$  isotopologues obtained  
396 from a controlled greenhouse, where atmospheric mixing and transport are largely reduced, to  
397 demonstrate the advantage of utilizing  $\Delta_{47}$  for flux partitioning between photosynthesis and  
398 respiration over other  $\text{CO}_2$  isotopologues. The data collected from other natural environments  
399 are also presented, compared, and discussed 

400 In urban and industrial places where anthropogenic emission is significant, all the three  
401 isotopic tracers, viz.,  $\delta^{13}\text{C}$ ,  $\delta^{18}\text{O}$ , and  $\Delta_{47}$ , provide information about the anthropogenic  
402 fraction of  $\text{CO}_2$  due to distinct values of their sources. For example in a traffic street, a two  
403 end member (background and anthropogenic  $\text{CO}_2$ ) mixing of any of these tracers may  
404 provide sufficiently good estimate of the anthropogenic fraction of  $\text{CO}_2$ . However, if a   
405 significant fraction of  $\text{CO}_2$  is respired from soil under  $\text{C}_3$  plants,  $\delta^{13}\text{C}$  cannot distinguish  
406 between the respired and anthropogenic sources.  $\delta^{18}\text{O}$  is always not applicable due to  
407 complexity of multiple oxygen-containing sources. Anthropogenic  $\text{CO}_2$  can also be  
408 quantified using radiocarbon ( $^{14}\text{C}$ ) as fossil fuels are highly depleted in  $^{14}\text{C}$  (Miller et al.,  
409 2012); however, it cannot distinguish difference between  $\text{CO}_2$  from two sources with modern  
410 carbon.

411 The un-catalyzed isotopic exchange time scale between  $\text{CO}_2$  and water is similar for both  
412  $\delta^{18}\text{O}$  and  $\Delta_{47}$  (e.g., see Affek, 2013), and therefore, we expect that the two provide similar  
413 information when  $\text{CO}_2$  in air simply exchanges with water. But it is not well understood if  
414 they behave similarly when biogeochemical processes such as photosynthesis and respiration  
415 are involved. We note that  $^{18}\text{O}$  is highly variable between reservoirs such as leaf water  
416 affected by evapotranspiration even when temperature variation is not very large. Thus,  $\Delta_{47}$   
417 can complement  $\delta^{18}\text{O}$  and  $^{14}\text{C}$  data to probe the associated processes in the  $\text{CO}_2$  cycling. A  
418 detailed analysis of the results from different locations is presented below. 

419

#### 420 4.1 Greenhouse $\text{CO}_2$

421 To minimize anthropogenic alteration and air mixing/transport and to maximize the  
422 variations of  $\text{CO}_2$  isotopologues by biogeochemical processes, a controlled greenhouse



423 provides an ideal environment. Diurnal variation **is** observed in  $[\text{CO}_2]$ ,  $\delta^{13}\text{C}$ ,  $\delta^{18}\text{O}$  (Figure 2),  
 424 and  $\Delta_{47}$  (Figure 3) in the greenhouse. Good correlations between  $[\text{CO}_2]$ ,  $\delta^{13}\text{C}$  and  $\delta^{18}\text{O}$   
 425 suggest common processes affecting all of them, and we believe they are photosynthesis and  
 426 respiration. Giving July 31<sup>st</sup> as an example, we estimate the rates of night-time respiration  
 427 and daytime photosynthetic uptake using the bulk isotopic compositions ( $\Delta_{47}$  which will be  
 428 discussed separately). The dimension of the greenhouse room is 8m, 5m and 5m (length,  
 429 width and height). The night-time respiration rate is then estimated to be about  $\sim 10$  ppmv per  
 430 hour (considering change of  $[\text{CO}_2]$  from 5:30 PM to 9:30 PM; Figure 2A), or  $\sim 4 \times 10^{13}$   
 431 molecules  $\text{cm}^{-2} \text{s}^{-1}$ . The increase of  $[\text{CO}_2]$  can be satisfactorily explained assuming  $\text{C}_3$   
 432 respiration as the main source of  $\text{CO}_2$  ( $\delta^{13}\text{C} \approx -26$  ‰; intercept in Figure 2D) added to the  
 433 background ( $-8.5$  ‰). Similarly, the same conclusion is also **arrived** by analyzing  $\delta^{18}\text{O}$  (the  
 434 respired  $\text{CO}_2$  is 30.68 ‰, intercept in Figure 2E, and background,  $\delta^{18}\text{O}$  of air  $\text{CO}_2$  outside, is  
 435 40 ‰). Thus, we conclude that the main factor that affects the changes in concentration as  
 436 well as the isotopic compositions in night-time is respiration.

437 The daytime net uptake rate can be estimated by taking the changes from early morning to  
 438 noon time; the  $[\text{CO}_2]$  reduces by 110 ppmv,  $\delta^{13}\text{C}$  increases by 3.46 ‰, and  $\delta^{18}\text{O}$  by 2.23 ‰ in  
 439 about six hours. The estimated net photosynthetic uptake is  $\sim 7 \times 10^{13}$  molecules  $\text{cm}^{-2} \text{s}^{-1}$ .  
 440 Neglecting respiration during daytime, the photosynthetic discrimination can be calculated  
 441 using the Rayleigh distillation model

$$442 \quad R = R_o f^{\alpha-1} \quad (3)$$

443 where  $R_o$  and  $R$  are the initial and photosynthesis modified  $^{13}\text{C}/^{12}\text{C}$  or  $^{18}\text{O}/^{16}\text{O}$  ratios,  
 444 respectively,  $f$  is the fraction of the material left, and  $\alpha$  is the fractionation factor. The  
 445 estimated discrimination in  $^{13}\text{C}$  defined by  $(\alpha-1)$ , following equation (3), is  $-15.3$  ‰, similar  
 446 to that expected for  $\text{C}_3$  type vegetation. For  $^{18}\text{O}$ , in addition to photosynthetic uptake, one has  
 447 to consider an additional effect due to temperature-dependent water- $\text{CO}_2$  equilibrium  
 448 fractionation. That is, the process decreases  $\delta^{18}\text{O}$  by  $\sim 0.2$  ‰ for an increase of  $1$  °C in  
 449 temperature (Brenninkmeijer et al., 1983); from morning to noon time, the temperature effect  
 450 reduces  $\delta^{18}\text{O}$  by  $-4.4$  ‰. Adding this factor to the observed change in  $\delta^{18}\text{O}$  yields a  
 451 discrimination of about  $-27$  ‰; the value becomes  $-9.5$  ‰, if this additional temperature-  
 452 dependence is ignored. The obtained discrimination factors for  $^{13}\text{C}$  and  $^{18}\text{O}$  are in good



453 agreement with those reported previously (Farquhar et al., 1989; Flanagan et al., 1997; Cuntz  
454 et al., 2003; Affek and Yakir, 2014).

455 Assuming ca. 1/3 of the CO<sub>2</sub> molecules in stomata are fixed photosynthetically, the  
456 remaining retro-diffuse back to the atmosphere (Farquhar and Lloyd, 1993), implying that the  
457 CO<sub>2</sub>-water isotopic exchange rate is  $\sim 2 \times 10^{14}$  molecules cm<sup>-2</sup> s<sup>-1</sup>, or 9 hours of oxygen isotope  
458 exchange time for CO<sub>2</sub> in the room. As a result, we do not expect that CO<sub>2</sub> reaches complete  
459 isotopic equilibrium with the substrate water in a few hours.  $\Delta_{47}$  values in the leftover CO<sub>2</sub>  
460 can be used to check the disequilibrium. The respired CO<sub>2</sub> are found to be always in  
461 thermodynamic equilibrium at the ambient temperature, shown by the  $\Delta_{47}$  values of CO<sub>2</sub> in  
462 the early morning and night-time (Figure 3A-3C) and that collected on a cloudy day with  
463 suppressed photosynthetic activity (Figure 3D). The close-thermodynamic equilibrium at  
464 reduced photosynthetic condition is also shown in Figure 4A that deviation from the expected  
465 is small. On sunny days, the [CO<sub>2</sub>],  $\delta^{13}\text{C}$ , and  $\delta^{18}\text{O}$  values change by 50-115 ppm, 2-4 ‰, and  
466 1.1-2.2 ‰, respectively, in a time period of  $\sim 5$  hours in the morning (Figure 2). Figure 3  
467 shows that the  $\Delta_{47}$  values retain the thermodynamic equilibrium values in the morning hours  
468 (until 9 AM) and deviate later on. The reduction and deviation in the  $\Delta_{47}$  values during the  
469 time period is  $\sim 0.05$  ‰ (Figures 3A-3C); the changes we believe are significant, as the values  
470 are much higher than the uncertainty of the measurements. We attribute this deviation to  
471 photosynthesis as it is seen when photosynthesis is strong. Strong influence of photosynthesis  
472 on  $\Delta_{47}$  was also reported previously (Eiler and Schauble, 2004). Photosynthesis as a source of  
473 disequilibrium was further shown recently by analyzing the clumped isotopes of O<sub>2</sub> (Yeung  
474 et al., 2005). Though enzymatic carbonic anhydrase catalyzes the water-CO<sub>2</sub> isotopic  
475 exchange toward equilibrium (Peltier et al., 1995; Cernusak et al., 2004), the reaction may  
476 not complete, limited by the enzymatic activity inside leaves; large variation in the activity of  
477 carbonic anhydrase in different vegetation types (C<sub>3</sub>, C<sub>4</sub>) or within the same type **is** observed  
478 (see Gillon and Yakir, 2001 and references therein). Furthermore, a box modeling by Eiler  
479 and Schauble (2004) demonstrated that gas diffusion through leaf stomata during  
480 photosynthesis fractionates the remaining air CO<sub>2</sub>  $\Delta_{47}$  values from the thermodynamic  
481 equilibrium set by leaf water. Mixing of more than one component can also cause change in  
482  $\Delta_{47}$  when bulk isotopic compositions of the components are different (Affek and Eiler, 2006),  
483 but this can easily be ruled out as it **is** not observed when photosynthesis **is** not very strong  
484 (Figure 3D). More rigorous investigations with controlled experiments using different plants





485 with diverse carbonic anhydrase activities are needed to resolve the issue. We note that no  
486 significant correlation between  $\delta^{18}\text{O}$  and  $\Delta_{47}$  is observed (Figure 3). Therefore, the plant  
487 photosynthesis decouples  $\Delta_{47}$  and  $\delta^{18}\text{O}$ ; in contrast, pure water- $\text{CO}_2$  isotopic exchange  
488 process shows that the two behave similarly as far as isotopic equilibration is concerned  
489 (Affek, 2013; Clog et al. 2015).

490 The  $\Delta_{47}$  thus serves as an independent tracer for studying photosynthesis. Though the  
491 deviation from equilibrium during photosynthesis is also observed in oxygen clumped  
492 isotopes [Yeung et al., 2015],  $\text{CO}_2$  and  $\text{O}_2$  are affected and produced from different processes  
493 and sources; the former is affected seriously by water (water- $\text{CO}_2$  isotopic exchange) while  
494 the latter is derived from water. We believe the analyses of the clumped isotopes for both  
495  $\text{CO}_2$  and  $\text{O}_2$  are of great importance in the atmospheric carbon cycling study, providing a new  
496 angle for tackling the chemistry chain in photosynthesis. More systematic study in controlled  
497 environments including leaf level experiments will help to better understand the role of  
498 photosynthesis on  $\Delta_{47}$ .

499

#### 500 4.2 Marine and coastal air $\text{CO}_2$

501 The concentration and  $\delta^{13}\text{C}$  values of marine air  $\text{CO}_2$  are close to the background atmospheric  
502 values reported at Mauna Loa, indicating little contribution from local/regional anthropogenic  
503 activities. The Keeling analysis for  $\delta^{13}\text{C}$  gives an intercept of  $-15.9 \pm 2.0$  ‰ (Figure 5A) which  
504 is the  $\delta^{13}\text{C}$  value of the source  $\text{CO}_2$  over the ocean. The  $\text{CO}_2$  released over ocean is mainly  
505 originated from the remineralization of organic matter in the deeper ocean. The  $\delta^{13}\text{C}$  value of  
506 which ranges between  $-20$  and  $-30$  ‰ in the tropical to subtropical oceans (Francois et al.,  
507 1993; Goericke and Fry, 1994), the intercept observed here is much higher than this range.  
508 possibility is that the remineralized  $\text{CO}_2$  gets equilibrated with the dissolved inorganic carbon  
509 before releasing. Again a complete equilibration of the  $\text{CO}_2$  with the dissolved inorganic  
510 carbon would lead to a  $\delta^{13}\text{C}$  value of released  $\text{CO}_2$  to be  $-9$  to  $-10$  ‰ (Mook, 1986; Boutton,  
511 1991; Zhang et al., 1995; Affek and Yakir, 2014), the observed value of the intercept is  
512 less than this. Therefore, we conclude that the  $\text{CO}_2$  produced in the deeper ocean is partially  
513 equilibrated with the dissolved inorganic carbon before releasing to the atmosphere.



514 The  $\delta^{18}\text{O}$  values of the surface sea water in the region in summer (July-September) and  
515 winter (December-February) are about  $-1.7\text{‰}$  and  $-0.6\text{‰}$  (Ye et al., 2014). The sea surface  
516 temperatures in the summer and winter are about  $28$  and  $24\text{ °C}$ , and the equilibrated  $\delta^{18}\text{O}$   
517 values of the atmospheric  $\text{CO}_2$  should be  $38.9\text{‰}$  and  $40.7\text{‰}$ , respectively (Brenninkmeijer  
518 et al., 1983). Our observed values lie in the range of  $40.4\text{‰}$  to  $41.0\text{‰}$  (Table 4), consistent  
519 with the isotopic equilibrium values with the surface water. Therefore, we conclude that  
520 oxygen isotopes in near surface air  $\text{CO}_2$  over ocean are close to the isotopic equilibrium with  
521 the surface sea water. This conclusion is further supported by the observed  $\Delta_{47}$  value. This is  
522 due to the same water- $\text{CO}_2$  exchange time for the two species (Affek, 2013; Clog et al.,  
523 2015). Comparing the greenhouse data above, we therefore conclude that  $\delta^{18}\text{O}$  and  $\Delta_{47}$   
524 respond differently when photosynthesis is the main governing factor and behave similarly  
525 when exchange occurs due to simple water- $\text{CO}_2$  equilibration. Though carbonic anhydrase  
526 are also present in the surface ocean and marine phytoplankton does photosynthesis,  $\delta^{18}\text{O}$  and  
527  $\Delta_{47}$  in air  $\text{CO}_2$  over the ocean show the values at thermodynamic equilibrium unlike  
528 greenhouse. The degree of deviation from thermodynamic equilibrium likely increases with  
529 the strength of photosynthesis. And normally the oceanic photosynthesis is less compared to  
530 the terrestrial plants. Therefore,  $\Delta_{47}$  can be used as a tracer for estimating terrestrial carbon  
531 uptake. Compared to  $\delta^{18}\text{O}$ ,  $\Delta_{47}$  is process sensitive and is not affected by the isotopic  
532 composition of substrate water. Given that the surface air temperature is better measured, we  
533 believe the clumped isotopes potentially provide good tracers for global carbon flux study  
534 involving  $\text{CO}_2$ , complementing the commonly used species like  $[\text{CO}_2]$ ,  $\delta^{13}\text{C}$ , and  $\delta^{18}\text{O}$ .

535 The isotopic values including  $\Delta_{47}$  in the two coastal stations are similar to those observed for  
536 the marine  $\text{CO}_2$ . The carbon Keeling analysis yields an intercept of  $-12.20 \pm 1.11\text{‰}$  (Figure  
537 5D), consistent with that for the marine  $\delta^{13}\text{C}$  (removing one outlier from Figure 5A gives an  
538 intercept of  $-13.3 \pm 1.0\text{‰}$ ). The  $\Delta_{47}$  values here are similar to the thermodynamic equilibrium  
539 with the sea surface water at the temperature of  $\sim 27\text{ °C}$  (Figure 7B). The recorded air  
540 temperature during the sampling period over the coasts varies between  $14$  and  $24\text{ °C}$  and is  
541 not reflected in the  $\Delta_{47}$  values. We note that the samples are collected from two open spaces  
542 in the coasts where strong north and northeasterly winds overwhelm, carrying air masses  
543 from the oceans towards the sampling locations (See Table S3 in Supporting Information).  
544 Therefore, we expect the major contribution is marine air with little influence from local



545 processes, which could occasionally cause deviation from the thermodynamic equilibrium  
546 values.

547

#### 548 **4.3 Car exhaust CO<sub>2</sub>**

549 The  $\Delta_{47}$  value of car exhaust CO<sub>2</sub> should reflect the temperature of fuel combustion inside the  
550 combustion chamber which is  $>800$  °C. However, the temperature estimated from  $\Delta_{47}$  is  
551 found to be  $283 \pm 18$  °C. It is likely that interaction of the sample CO<sub>2</sub> with the condensed  
552 water in the exhaust pipe modifies the  $\Delta_{47}$  value: during sample collection, we observed that  
553 the exhaust gas contains a large amount of water vapor and some of which get condensed on  
554 the exhaust pipe and the front part of the magnesium perchlorate column. Precautions, such  
555 as opening the evacuated flask for a short time ( $<1$  min) and careful holding of the sampling  
556 tube inside the exhaust pipe without touching the wall of the pipe, are taken to minimize  
557 CO<sub>2</sub>-water interaction during sample collection.

558 The higher  $\Delta_{47}$  value for the exhaust CO<sub>2</sub> indicates isotopic re-equilibration of CO<sub>2</sub> with  
559 water in the stream of the exhaust gas and inside catalytic converter. Also supported by the  
560 observed enriched  $\delta^{18}\text{O}$  than atmospheric O<sub>2</sub>; the oxygen atoms in the two most abundant  
561 species, water and CO<sub>2</sub> here, are mostly originated from atmospheric O<sub>2</sub> and are expected to  
562 inherit the isotopic composition of atmospheric O<sub>2</sub>. Formally isotopes in CO<sub>2</sub> do not  
563 exchange with water vapor, but inside catalytic converter, exchange may take place on the  
564 surface of the catalyst at certain temperature (which is usually much less than the combustion  
565 temperature). Affek and Eiler (2007) also observed elevated  $\Delta_{47}$  values for car exhausts and  
566 estimated a temperature of CO<sub>2</sub> production to be  $\sim 200$  °C. The temperature estimated here  
567 is significantly higher than that observed by Affek and Eiler (2007). Difference could be due to  
568 different car models and the variations in the temperatures of the catalytic converters from car  
569 to car.

570

#### 571 **4.4 Urban and sub-urban air CO<sub>2</sub>**

572 A significant fraction of anthropogenic CO<sub>2</sub> is present in the air CO<sub>2</sub> over the urban site,  
573 indicated by the [CO<sub>2</sub>] as well as isotopic compositions including  $\Delta_{47}$ . Limits to the



574 anthropogenic contribution can be estimated following a two component mixing:  $\delta =$   
 575  $f_{\text{anth}} \times \delta_{\text{anth}} + (1 - f_{\text{anth}}) \times \delta_{\text{bgd}}$ , where  $\delta$ 's can be  $\delta^{13}\text{C}$  or  $\delta^{18}\text{O}$  or  $\Delta_{47}$  and  $f$ 's, the corresponding  
 576 weighting factor, and subscripts 'anth' and 'bgd' refer to anthropogenic and background,  
 577 respectively. We take the 'anthropogenic' and 'background' end member isotopic  
 578 compositions from the car exhaust (Table 3) and marine  $\text{CO}_2$  (Table 4), respectively.  
 579 Assuming that the excess in  $[\text{CO}_2]$  above the background is originated from vehicular  
 580 emissions, the values of the  $\delta^{13}\text{C}$ ,  $\delta^{18}\text{O}$ , and  $\Delta_{47}$  in the urban site obtained using the mixing  
 581 equation are -12.26 ‰, 37.68 ‰, and 0.791 ‰, respectively, which are similar to those  
 582 observed (Table 5).  $\Delta_{47}$  is not a conserved quantity and a linear mixing is not valid when the  
 583 bulk isotopic compositions of the components are widely different. In the present case, the  
 584 isotopic compositions of the two components are not drastically different and fraction of  
 585 anthropogenic  $\text{CO}_2$  is much less ( $<1/4$ ) than the background  $\text{CO}_2$ , and hence the error due to  
 586 linear approximation is smaller than the uncertainty of measurement.

587 No systematic diurnal or temporal trend is observed in the  $\Delta_{47}$  values in sub-urban  $\text{CO}_2$   
 588 during the sampling period (Figure 7C) though a weak trend is seen in  $\delta^{13}\text{C}$  and  $\delta^{18}\text{O}$  (Figure  
 589 6), furthermore demonstrating that  $\Delta_{47}$  behaves differently from  $[\text{CO}_2]$ ,  $\delta^{13}\text{C}$ , and  $\delta^{18}\text{O}$ .  
 590 Almost all measured  $\Delta_{47}$  values are lower than that expected at the ambient temperature  
 591 except two days: 9<sup>th</sup> November, 2013 and 3<sup>rd</sup> February, 2014.  $\delta^{13}\text{C}$  values are also slightly  
 592 lower than the background values. The reduced values of  $\Delta_{47}$  could be due to contribution of  
 593  $\text{CO}_2$  from combustion processes which produce  $\text{CO}_2$  with low  $\Delta_{47}$  values as discussed in  
 594 Section 4.3. We estimate the contribution of local anthropogenic emissions in  $\delta^{13}\text{C}$  and  $\Delta_{47}$   
 595 using the two components mixing discussed above. The components are the background air  
 596  $\text{CO}_2$  and car exhausts. The expected  $\delta^{13}\text{C}$  and  $\Delta_{47}$  values of the mixture are -9.1 ‰ and 0.92  
 597 ‰, respectively. The observed  $\Delta_{47}$  value is significantly different from that estimated from  
 598 simple two component mixing, though it is not different for  $\delta^{13}\text{C}$ , suggesting other processes  
 599 like photosynthesis present in affecting  $\Delta_{47}$ . After subtracting the local anthropogenic  
 600 contribution from the observed  $\Delta_{47}$  values, a difference of  $\sim 0.026$  ‰ between the observed  
 601 and estimated remains for sub-urban station and it disappears for urban station (see Table S4  
 602 in Supporting Information). This is not obvious in  $\delta^{13}\text{C}$  probably due to larger variation. The  
 603 lower  $\Delta_{47}$  values in sub-urban station could possibly be due to kinetic effect during  
 604 photosynthetic assimilation, partial contribution of marine air, or a combination of the two. The  
 605 marine air in the vicinity of Taiwan, which is at thermodynamic equilibrium with the surface



606 sea water as discussed earlier, may contribute partially to the air CO<sub>2</sub> at the sampling site.  
607 Varying contribution of marine air could explain the lower  $\Delta_{47}$  values to some extent. The  
608 respired CO<sub>2</sub> is in thermodynamic equilibrium as shown above (Section 4.1). Therefore, the  
609 most plausible cause for observed deviation in the  $\Delta_{47}$  values that cannot be accounted for by  
610 anthropogenic and marine alterations is photosynthesis, as discussed earlier for greenhouse  
611 CO<sub>2</sub>. This is not unreasonable, as the Academia Sinica Campus is surrounded by thick  
612 greeneries.


613 On 9<sup>th</sup> Nov, 2013 and 3<sup>rd</sup> February, 2014, the  $\Delta_{47}$  values are close to that expected at  
614 thermodynamic equilibrium (Figure 7C). The  $\Delta_{47}$  values on 9<sup>th</sup> November are not very  
615 different from the values reported for the previous or next days. However, the calculated  
616 thermodynamic equilibrium values on that day are relatively low due to higher ambient  
617 temperatures (Figure 7C). On 3<sup>rd</sup> February, 2014, the  $\Delta_{47}$  values are higher and comparable  
618 to the thermodynamic equilibrium values expected at ambient temperatures. A likely  
619 explanation is that on that day relatively strong wind from the southern land (Table S3 in  
620 Supporting Information) contributed the air CO<sub>2</sub>. Higher  $\Delta_{47}$  values are due to mixing of  
621 the local air with that transported from the south of Taipei.

622


#### 623 4.5 Forest, grassland and high mountain air CO<sub>2</sub>

624 An elevated CO<sub>2</sub> concentration and low  $\delta^{13}\text{C}$  and  $\delta^{18}\text{O}$  values indicate significant contribution  
625 of respiration and/or anthropogenic CO<sub>2</sub> in the forest station (Table 5) near the Academia  
626 Sinica Campus. Though the samples are collected at 10-11 AM under bright sunlight, the  
627 vegetation is so dense that little sunlight reached the ground. As a result, photosynthesis is  
628 weakened at the ground level. Also poor circulation of air due to presence of high hills on  
629 the three sides of the sampling spot makes the site nearly isolated from the surroundings. The  
630  $\Delta_{47}$  values are similar to the thermodynamic equilibrium expected at the ambient  
631 temperatures except on 11<sup>th</sup> August, 2015 on which a significantly higher  $\Delta_{47}$  value is  
632 observed (Figure 7F). The higher value is likely due to the influence of the super Typhoon  
633 Soudelor which passed over Taipei during 8-10 August, 2015 causing a decrease in  
634 temperature by 3-4 °C and air masses mixing in a larger spatial scale.



635 In the grassland station in Taipei city, the Keeling plot for  $\delta^{13}\text{C}$  gives an intercept of -  
636  $17.0 \pm 1.0$  ‰ (Figure 5D). This indicates some sources of  $\text{CO}_2$  with higher  $\delta^{13}\text{C}$  values  
637 compared to the most expected sources, namely,  $\text{C}_3$  vegetation and vehicle emission with a  
638  $\delta^{13}\text{C}$  value of  $\sim -27$  ‰. The samples are collected just above the surface of the grasses.  
639 Tropical warm grasses are mainly  $\text{C}_4$  type with  $\delta^{13}\text{C}$  in the range of -9 to -19 ‰ and a global  
640 average of -13 ‰ (Deines, 1980). We measured  $\delta^{13}\text{C}$  values of a few grass samples and  
641 found values in the range of -15 to -17 ‰. The soil and grass respired  $\text{CO}_2$  with higher  $\delta^{13}\text{C}$   
642 contributed significantly to the near surface  $\text{CO}_2$ , resulting in an elevated intercept of -17 ‰.  
643 The concentration is sometimes observed to be less than the background level, probably due  
644 to strong  $\text{CO}_2$  uptake by plants. The temperature gradually decreased from 26 to 20 °C during  
645 the consecutive three days and clumped isotope followed similar trend, reflecting the  
646 influence of temperature on  $\text{CO}_2$   $\Delta_{47}$  and rapid equilibration with the leaf and surface waters.  
647 The low value observed on the second day is probably due to plumes of vehicle exhausts,  
648 supported by the elevated level in  $[\text{CO}_2]$  and depletion in  $\delta^{13}\text{C}$  and  $\delta^{18}\text{O}$  (Table 5) 

649 For high mountain  $\text{CO}_2$ , the  $\Delta_{47}$  value (Table 5) is lower than that expected at  $\sim 10$  °C, the  
650 ambient temperature at the top of the mountain site during sampling. The  $\Delta_{47}$  values are  
651 similar to that observed in the plain and over the ocean. We note that during the sampling  
652 period, the site was affected significantly by winter monsoons. HYSPLIT 24 hours back  
653 trajectory shows marine origin of air (not shown) during the sampling time. The air  $\text{CO}_2$  on  
654 the mountain probably does not get sufficient time to isotopically equilibrate with the local  
655 surface and leaf water but show the signature of the marine  $\text{CO}_2$ .

656 The deviations in  $\Delta_{47}$  from the thermodynamic equilibrium values in different atmospheric  
657 environments and processes are summarized in Figure 8 . It is obvious that the urban and sub-  
658 urban  $\text{CO}_2$  deviate the most towards lower  $\Delta_{47}$  values, mainly contributed by  $\text{CO}_2$  originated  
659 from high temperature combustions, i.e., vehicular emissions. The respired  $\text{CO}_2$  are always in  
660 close thermodynamic equilibrium at the ambient temperature. On the other hand,  $\text{CO}_2$   
661 affected by strong photosynthesis show significant deviation from the thermodynamic  
662 equilibrium values. Kinetic isotopic fractionation during diffusion of  $\text{CO}_2$  in and out of leaf  
663 stomata is a probable reason.

664

## 665 5. Summary



666 We presented a compilation of  $\Delta_{47}$  analyses for car exhaust, greenhouse and air CO<sub>2</sub> over a  
667 wide variety of interactions in tropical and sub-tropical regions including marine, coastal,  
668 urban, sub-urban, forest, and high mountain environments. Car exhaust, urban, sub-urban and  
669 greenhouse air CO<sub>2</sub> significantly deviate from the thermodynamic equilibrium values. While  
670 respired CO<sub>2</sub> is in thermodynamic equilibrium with leaf and soil surface waters,  
671 photosynthesis significantly deviates the  $\Delta_{47}$  values from the thermodynamic equilibrium

672 The  $\Delta_{47}$  values in urban and sub-urban air CO<sub>2</sub> are lower than that expected under  
673 thermodynamic equilibrium at the ambient temperature. The deviation is mainly due to  
674 contributions from fossil fuel emissions and to some extent due to photosynthesis especially  
675 in regions with dense vegetation. We expect  $\Delta_{47}$  can shed light on the estimation of  
676 anthropogenic contribution to the atmospheric CO<sub>2</sub> and the activity of photosynthesis. The  
677 latter deserves further investigation, to establish how exactly  $\Delta_{47}$  is affected by  
678 photosynthesis, before the tracer can be used for estimating gross primary productivity

679

#### 680 **Data availability**

681 All the data used in the manuscript are also presented in the form of Tables.

#### 682 **Acknowledgement**

683 We thank Dr. Chung-Ho Wang for providing waters with different  $\delta^{18}\text{O}$ , Institute of Earth  
684 Sciences, Academia Sinica for providing laboratory space, Mr. Frank Lin for helping  
685 sampling in greenhouse, Dr. Jia-Lin Wang and Dr. Chang-Feng Ou-Yang for calibrating  
686 compressed air cylinder, Mr. Hao-Wei Wei for collecting air at the campus of National  
687 Taiwan University and Mr. Wei-Kang Ho for collecting oceanic CO<sub>2</sub> and helping in  
688 laboratory setups. Special thanks to Prof. S. K. Bhattacharya and Dr. Sasadhar Mahata for  
689 helpful discussion. This work is supported by the Ministry of Science and Technology  
690 (MOST-Taiwan) grants 101-2628-M-001-001-MY4 and 103-2111-M-001-006 to Academia  
691 Sinica and Academia Sinica Career Development Award and MOST 103-2119-M-002-022 to  
692 National Taiwan University.

693

694 **References**

- 695 Affek H. P., and Eiler J. M.: Abundance of mass 47 CO<sub>2</sub> in urban air, car exhaust, and human  
696 breath, *Geochim. Cosmochim. Acta*, 70, 1–12, 2006.
- 697 Affek H. P., Xu X., and Eiler J. M.: Seasonal and diurnal variations of <sup>13</sup>C<sup>18</sup>O<sup>16</sup>O in air:  
698 Initial observations from Pasadena CA, *Geochim. Cosmochim. Acta*, 71, 5033–5043,  
699 2007.
- 700 Affek H. P., and Yakir D.: The stable isotopic composition of atmospheric CO<sub>2</sub>, *Treaties of*  
701 *Geochemistry*, 5, 179–212, 2014.
- 702 Affek, H. P.: Clumped isotopic equilibrium and the rate of isotope exchange between CO<sub>2</sub>  
703 and water, *Am. J. Sci.* 313 (4), 309–325, 2013.
- 704 Barkan E., and Luz B.: High precision measurements of <sup>17</sup>O/<sup>16</sup>O and <sup>18</sup>O/<sup>16</sup>O ratios in H<sub>2</sub>O,  
705 *Rapid Commun. Mass Spectrom.*, 19, 3737–3742, 2005.
- 706 Brenninkmeijer, C. A. M., Kraft, P and Mook, W. G.: Oxygen isotope fractionation between  
707 CO<sub>2</sub> and H<sub>2</sub>O, *Isot. Geosci.*, 1, 181–190, 1983.
- 708 Boutton, T. W.: Stable carbon isotope ratios of natural materials. II. Atmospheric, terrestrial,  
709 marine, and freshwater environments, in *Carbon Isotope Techniques*, edited by D. C.  
710 Coleman and B. Fry, pp. 173–185, Academic Press, New York, 1991.
- 711 Bowling, D. R., Ballantyne, A. P., Miller, J. B., Burns, S. P., Conway, T. J., Menzer, O.,  
712 Stephens, B. B., and Vaughn, B. H.: Ecological processes dominate the <sup>13</sup>C land  
713 disequilibrium in a Rocky Mountain subalpine forest, *Global Biogeochem. Cycles*, 27,  
714 doi:10.1002/2013GB004686, 2014.
- 715 Cernusak, L. A., Farquhar, G. D., Wong, S. C., and Williams, H. S.: Measurement and  
716 Interpretation of the Oxygen Isotope Composition of Carbon Dioxide Respired by  
717 Leaves in the Dark, *Plant Physiology*, 136, 3350–3363, 2004.
- 718 Ciais, P., Denning, A. S., Tans, P. P., Berry, J. A., Randall, D. A., Collatz, G. J., Sellers, P.  
719 J., White, J. W. C., Trolier, M., Meijer, H. A. J., Francey, R. J., Monfray, P., and  
720 Heimann, M.: A three-dimensional synthesis study of δ<sup>18</sup>O in atmospheric CO<sub>2</sub>. 1.  
721 Surface fluxes, *J. Geophys. Res. -Atm.*, 102, 5857–5872, 1997.
- 722 Ciais, P., Tans, P. P., Trolier, M., White, J. W. C., and Francey, R. J.: A large northern-  
723 hemisphere terrestrial CO<sub>2</sub> sink indicated by the <sup>13</sup>C/<sup>12</sup>C ratio of atmospheric CO<sub>2</sub>,  
724 *Science*, 269, 1098–1102, 1995a.





- 725 Ciais, P., Tans, P. P., White, J. W. C., Trolier, M., Francey, R. J., Berry, J. A., Randall, D.  
726 R., Sellers, P. J., Collatz, J. G., and Schimel, D. S.: Partitioning of ocean and land  
727 uptake of CO<sub>2</sub> as inferred by δ<sup>18</sup>O measurements from the NOAA Climate Monitoring  
728 and Diagnostics Laboratory Global Air Sampling Network, *J. Geophys. Res.*, 100,  
729 5051–5070, 1995b.
- 730 Clog, M., Stolper, D., and Eiler, J. M.: Kinetics of CO<sub>2</sub>(g)–H<sub>2</sub>O(1) isotopic exchange,  
731 including mass 47 isotopologues, *Chem. Geol.*, 395, 1–10, 2015.
- 732 Cuntz, M., Ciais, P., Hoffmann, G., Allison, C. E., Francey, R. J., Knorr, W., Tans, P. P.,  
733 White, J. W. C., and Levin, I.: A comprehensive global three-dimensional model of  
734 δ<sup>18</sup>O in atmospheric CO<sub>2</sub>: 2. Mapping the atmospheric signal, *J. Geophys. Res.*, 108,  
735 (D17), DOI: 10.1029/2002jd003153, 2003.
- 736 Deines, P.: The isotopic composition of reduced organic carbon, in: *Handbook of*  
737 *Environmental Isotope Geochemistry, 1. The Terrestrial Environment*, edited by Fritz,  
738 P. and Fontes, J. C. Elsevier, 329–406, 1980.
- 739 Dennis, K. J., Affek, H. P., Passey, B. H., Schrag, D. P., and Eiler, J. M.: Defining an  
740 absolute reference frame for ‘clumped’ isotope studies of CO<sub>2</sub>, *Geochim. Cosmochim.*  
741 *Acta*, 75, 7117–7131, 2011.
- 742 Drake, J. E., et al.: Increases in the flux of carbon belowground stimulate nitrogen uptake and  
743 sustain the long-term enhancement of forest productivity under elevated CO<sub>2</sub>, *Ecology*  
744 *Letters*, 14, 349–357, 2011.
- 745 Eiler, J. M. and Schauble, E.: <sup>18</sup>O<sup>13</sup>C<sup>16</sup>O in Earth’s atmosphere, *Geochim. Cosmochim. Acta*,  
746 68, 4767–4777, 2004.
- 747 Farquhar, G. D., Ehleringer, J. R., and Hubick, K. T.: Carbon isotope discrimination and  
748 photosynthesis, *Annu. Rev. Plant. Physiol. Plant Mol. Biol.*, 40, 503–537, 1989.
- 749 Farquhar, G. D. and Lloyd, J.: Carbon and oxygen isotope effects in the exchange of carbon  
750 dioxide between plants and the atmosphere, in: *Stable isotopes and plant carbon-water*  
751 *relations*, edited by J. R. Ehleringer, A. E. Hall, and G. D. Farquhar, Academic Press,  
752 New York, 47–70, 1993.
- 753 Flanagan, L. B., Brooks, J. R., Varney, G. T., Ehleringer, J. R.: Discrimination against  
754 C<sup>18</sup>O<sup>16</sup>O during photosynthesis and the oxygen isotope ratio of respired CO<sub>2</sub> in boreal  
755 forest ecosystems, *Global Biogeochem. Cycles*, 11(1), 83–98, 1997.
- 756 Francey, R. J. and Tans, P. P.: Latitudinal variation in O-18 of atmospheric CO<sub>2</sub>, *Nature*, 327,  
757 495–497, 1987.



- 758 Francey, R. J., Tans, P. P., Allison, C. E., Enting, I. G., White, J. W. C. and Trolrier, M.:  
759 Changes in oceanic and terrestrial carbon uptake since 1982, *Nature*, 373 (6512), 326–  
760 330, 1995.
- 761 Francois, R., Altabet, M. A., Goericke, R., McCorckle, D. C., Brunet, C., and Poisson, A.:  
762 Changes in the  $\delta^{13}\text{C}$  of surface water particulate organic matter across the subtropical  
763 convergence in the SW Indian Ocean, *Global Biogeochem. Cycles*, 7(3), 627–644,  
764 1993.
- 765 Ghosh, P., Adkins, J., Affek, H. P., Balta, B., Guo, W., Schauble, E., Schrag, D., and Eiler, J.  
766 M.:  $^{13}\text{C}$ – $^{18}\text{O}$  bonds in carbonate minerals: a new kind of paleothermometer, *Geochim.*  
767 *Cosmochim. Acta*, 70, 1439–1456, 2006.
- 768 Gillon, J., Yakir, D.: Influence of carbonic anhydrase activity in terrestrial vegetation on  
769 the  $^{18}\text{O}$  content of atmospheric  $\text{CO}_2$ , *Science* 291, 2584–2587, 2001.
- 770 Goericke, R. and Fry, B.: Variations of marine plankton  $\delta^{13}\text{C}$  with latitude, temperature, and  
771 dissolved  $\text{CO}_2$  in the world ocean, *Global Biogeochem. Cycles*, 8(1), 85–90, 1994.
- 772 He, B., Olack, G. A., and Colman, A. S.: Pressure baseline correction and high-precision  $\text{CO}_2$   
773 clumped isotope ( $\Delta_{47}$ ) measurements in bellows and micro-volume modes, *Rapid*  
774 *Comm. Mass Spec.*, 26, 2837–2853, 2012.
- 775 Hoag, K. J., Still, C. J., Fung, I. Y., and Boering, K. A.: Triple oxygen isotope composition of  
776 tropospheric carbon dioxide as a tracer of terrestrial gross carbon fluxes, *Geophys.*  
777 *Res. Lett.*, 32, L02802, doi:10.1029/2004GL021011, 2005.
- 778 Hofmann, M. E. G., Horváth, B., and Pack, A.: Triple oxygen isotope equilibrium  
779 fractionation between carbon dioxide and water, *Earth Planet. Sci. Lett.*, 319–320,  
780 159–164, 2012.
- 781 Huntington, K. W., Eiler, J. M., Affek, H. P., Guo, W., Bonifacie, M., Yeung, L. Y.,  
782 Thiagranjan, N., Passey, B., Tripathi, A., Daëron, M., and Came, R.: Methods and  
783 limitations of 'clumped'  $\text{CO}_2$  isotope ( $\Delta_{47}$ ) analysis by gas-source isotope ratio  
784 mass spectrometry, *J. Mass Spectrom.*, 44(9), 1318–29. doi: 10.1002/jms.1614, 2009.
- 785 Ito, A.: A global-scale simulation of the  $\text{CO}_2$  exchange between the atmosphere and the  
786 terrestrial biosphere with a mechanistic model including stable carbon isotopes, 1953–  
787 1999, *Tellus* 55B, 596–612, 2003.
- 788 Kroopnick, P., and Craig, H.: Atmospheric oxygen – Isotopic composition and solubility  
789 fraction, *Science*, 175, 54–55, 1972.



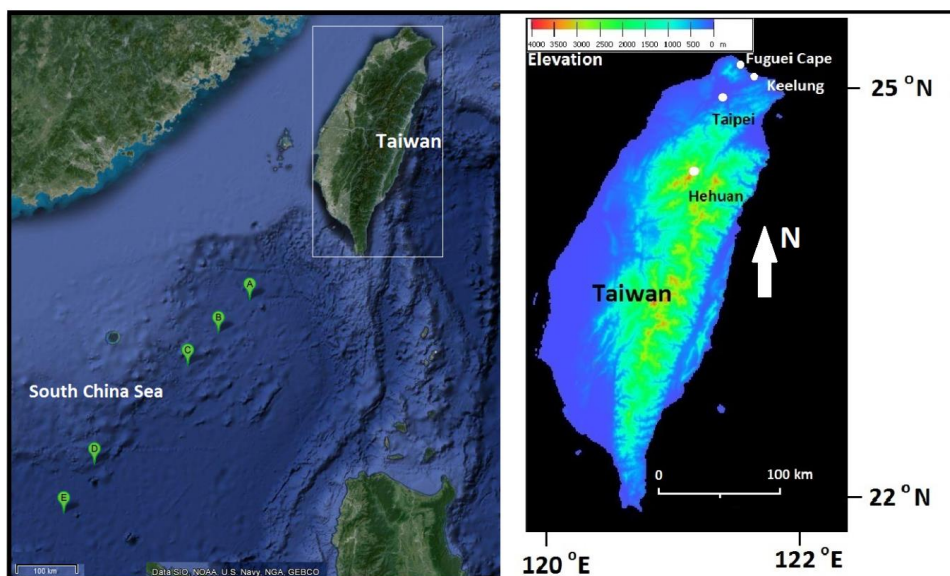
- 790 Landais, A., Barkan, E., Yakir, D., and Luz, B.: The triple isotopic composition of oxygen in  
791 leaf water, *Geochim. Cosmochim. Acta*, 70, 4105-4155, 2006.
- 792 Laskar, A. H., Huang, J. C., Hsu, S. C., Bhattacharya, S. K., Wang, C. H., and Liang, M. C.:  
793 Stable isotopic composition of near surface atmospheric water vapor and rain–vapor  
794 interaction in Taipei, Taiwan, *J. Hydrol*, 519, 2091-2100, 2014.
- 795 Mahata, S., Bhattacharya, S. K., Wang, C. H., and Liang, M. C.: An improved  $\text{CeO}_2$  method  
796 for high-precision measurements of  $^{17}\text{O}/^{16}\text{O}$  ratios for atmospheric carbon dioxide,  
797 *Rapid Commun. Mass Spectrom.*, 26, 1909–1922, 2012.
- 798 Miller, J. B., Lehman, S. J., Montzka, S. A., et al.: Linking emissions of fossil fuel  $\text{CO}_2$  and  
799 other anthropogenic trace gases using atmospheric  $^{14}\text{CO}_2$ , *J. Geophys. Res.*, 117,  
800 D08302, doi:10.1029/2011JD017048, 2012.
- 801 Mook, W. G.:  $^{13}\text{C}$  in atmospheric  $\text{CO}_2$ , *Neth. J. Sea Res.*, 20, 211-23, 1986.
- 802 Murayama, S., Takamura, C., Yamamoto, S., Saigusa, N., Morimoto, S., Kondo, H.,  
803 Nakazawa, T., Aoki, S., Usami, T., and Kondo, M.: Seasonal variations of atmospheric  
804  $\text{CO}_2$ ,  $\delta^{13}\text{C}$ , and  $\delta^{18}\text{O}$  at a cool temperate deciduous forest in Japan: Influence of Asian  
805 monsoon, *J. Geophys. Res.*, 115, D17304, doi:10.1029/2009JD013626, 2010.
- 806 Newman, S., Xu, X., Affek, H. P., Stolper, E., Epstein, S.: Changes in mixing ratio and  
807 isotopic composition of  $\text{CO}_2$  in urban air from the Los Angeles basin, California,  
808 between 1972 and 2003, *J. Geophys. Res.*, 113, D23304, doi:10.1029/2008JD009999,  
809 2008.
- 810 Popa, M. E., Vollmer, M. K., Jordan, A., Brand, W. A., Pathirana, S. L., Rothe, M.,  
811 Röckmann, T.: Vehicle emissions of greenhouse gases and related tracers from a  
812 tunnel study:  $\text{CO}:\text{CO}_2$ ,  $\text{N}_2\text{O}:\text{CO}_2$ ,  $\text{CH}_4:\text{CO}_2$ ,  $\text{O}_2:\text{CO}_2$  ratios, and the stable isotopes  $^{13}\text{C}$   
813 and  $^{18}\text{O}$  in  $\text{CO}_2$  and  $\text{CO}$ , *Atmos. Chem. Phys.*, 14, 2105–2123, 2014.
- 814 Peltier, G., Cournac, L., Despax, V., Dimon, B., Fina, L., Genty, B., and Rumeau, D.:  
815 Carbonic anhydrase activity in leaves as measured in vivo by  $^{18}\text{O}$  exchange between  
816 carbon dioxide and water, *Planta*, 196, 732-739, 1995.
- 817 Peng, T., Wang, H. C., and Huang, C.: Stable isotopic characteristic of Taiwan's  
818 precipitation: a case study of western Pacific monsoon region, *Earth Planet. Sci. Lett.*,  
819 289 (3–4), 357–366, 2010.
- 820 Peylin, P., Ciais, P., Denning, A. S., Tans, P. P., Berry, J. A., and White, J. W. C.: A 3-  
821 dimensional study of  $\delta^{18}\text{O}$  in atmospheric  $\text{CO}_2$ : contribution of different land



- 822 ecosystems, *Tellus Series B—Chemical and Physical Meteorology*, 51(3), 642–667,  
823 1999.
- 824 Tans, P. P., Berry, J. A., and Keeling, R. F.: Oceanic  $^{13}\text{C}/^{12}\text{C}$  observations: A new window on  
825 ocean  $\text{CO}_2$  uptake, *Global Biogeochem. Cycles*, 7(2) 353–368, 1993.
- 826 Thiemens, M. H., Chakraborty, S., Jackson, T. L.: Decadal  $\Delta^{17}\text{O}$  record of tropospheric  $\text{CO}_2$ :  
827 Verification of a stratospheric component in the troposphere, *J. Geophys. Res.*, 119,  
828 6221–6229, 2014.
- 829 Wang, Z., Schauble, E. A., and Eiler, J. M.: Equilibrium thermodynamics of multiply  
830 substituted isotopologues of molecular gases, *Geochim. Cosmochim. Acta*, 68(23),  
831 4779–4797, 2004.
- 832 Welp, L. R., Keeling, R. F., Meijer, H. A. J., Bollenbacher, A. F., Piper, S. C., Yoshimura,  
833 K., Francey, R. J., Allison, C. E., and Wahlen, M.: Interannual variability in the  
834 oxygen isotopes of atmospheric  $\text{CO}_2$  driven by El Niño, *Nature*, 477, 579–582, 2011.
- 835 Yakir, D., and Wang, X. F.: Fluxes of  $\text{CO}_2$  and water between terrestrial vegetation and the  
836 atmosphere estimated from isotope measurements, *Nature*, 380, 515–517, 1996.
- 837 Ye, F., Deng, W., Xie, L., Wei, G., and Jia, G.: Surface water  $\delta^{18}\text{O}$  in the marginal China seas  
838 and its hydrological implications. *Estuarine, Coastal and Shelf Science* 147, 25–31,  
839 2014.
- 840 Yeung, L. Y. et al.: Large and unexpected enrichment in stratospheric  $^{16}\text{O}^{13}\text{C}^{18}\text{O}$  and its  
841 meridional variation, *Proc. Nat. Acad. Sci. USA*, 106(28), 11496–11501, 2009.
- 842 Yeung, L. Y., Ash, J. L., and Young, E. D.: Biological signatures in clumped isotopes of  $\text{O}_2$ ,  
843 *Science* 348, 431–434, 2015.
- 844 Zhang, J., P. Quay, D., and Wilbur, D. O.: Carbon isotope fractionation during gas-water  
845 exchange and dissolution of  $\text{CO}_2$ , *Geochim. Cosmochim. Acta.*, doi:10.1016/0016-  
846 7037(95)91550-d, 1995.
- 847



848 **Figures**

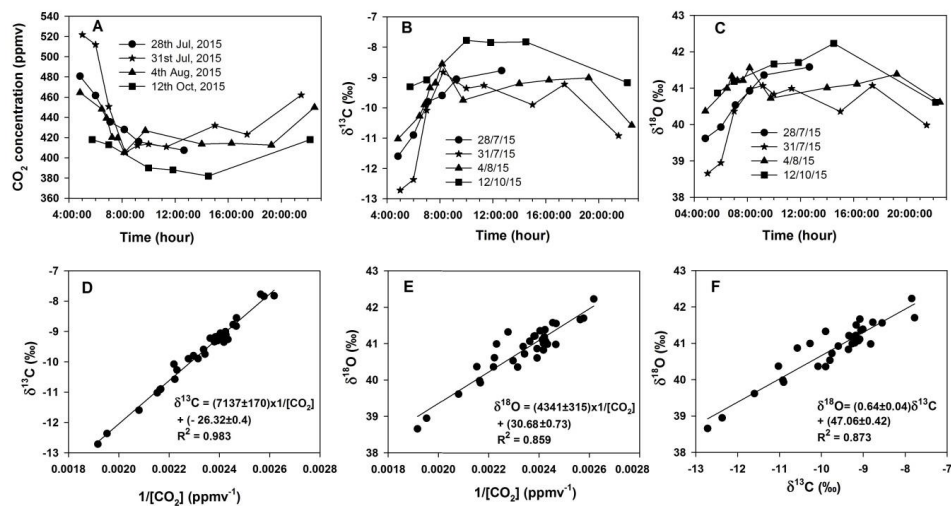


849

850 Figure 1. Map of Taiwan and South China Sea with the locations of air sampling. Marine air  
851 CO<sub>2</sub> sampling stations (A to E) in the South China Sea are shown on the left. Fuguei Cape  
852 and Keelung are two coastal stations, urban site (Roosevelt Road) and grassland (National  
853 Taiwan University Campus) are located at the centre of Taipei City and sub-urban site  
854 (Academia Sinica Campus) at the outskirts of the city and Hehuan is a high mountain station  
855 (~3000 m a.s.l.); all are shown on the right.

856

857



858

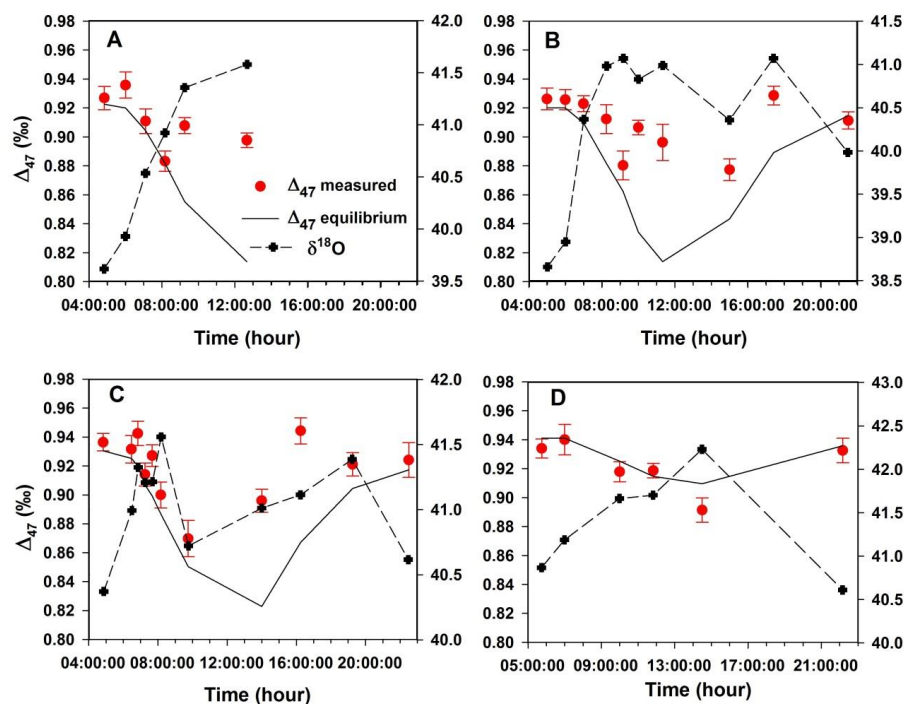
859 Figure 2. Top panels show the diurnal variation of (A) concentration, (B) δ<sup>13</sup>C, and (C) δ<sup>18</sup>O

860 of CO<sub>2</sub> sampled in the greenhouse. Bottom panels are the Keeling plots for (D) δ<sup>13</sup>C and (E)

861 δ<sup>18</sup>O and (F) scatter plot of δ<sup>13</sup>C and δ<sup>18</sup>O to show their covariance.

862

863



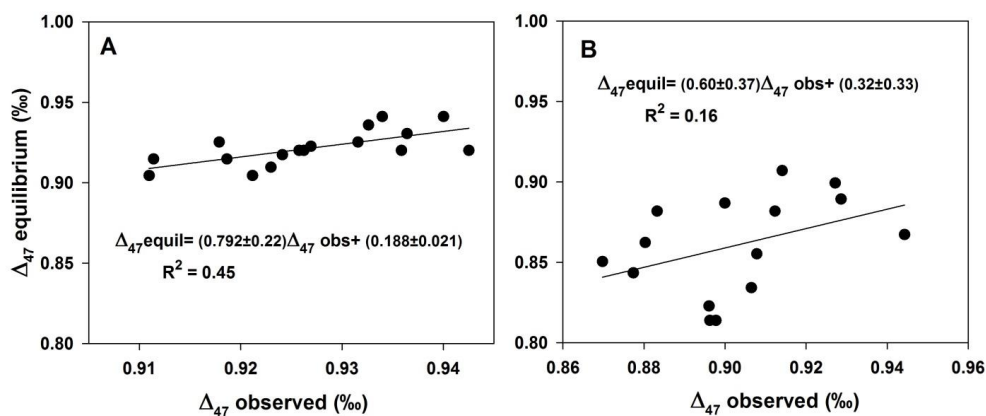
864

865 |Figure 3. Diurnal variation of the  $\Delta_{47}$  and  $\delta^{18}\text{O}$  values in the greenhouse for samples collected  
866 on four days of 2015: (A) 28<sup>th</sup> July, (B) 31<sup>st</sup> July, (C) 4<sup>th</sup> August, and (D) 12<sup>th</sup> October. The  
867 first three days (A-C) were bright sunny days and the last one (D) on a cloudy day with  
868 covered rooftop (see texts for details). The error bars are 1 standard error associated with the  
869 measurements.

870

871

872



873

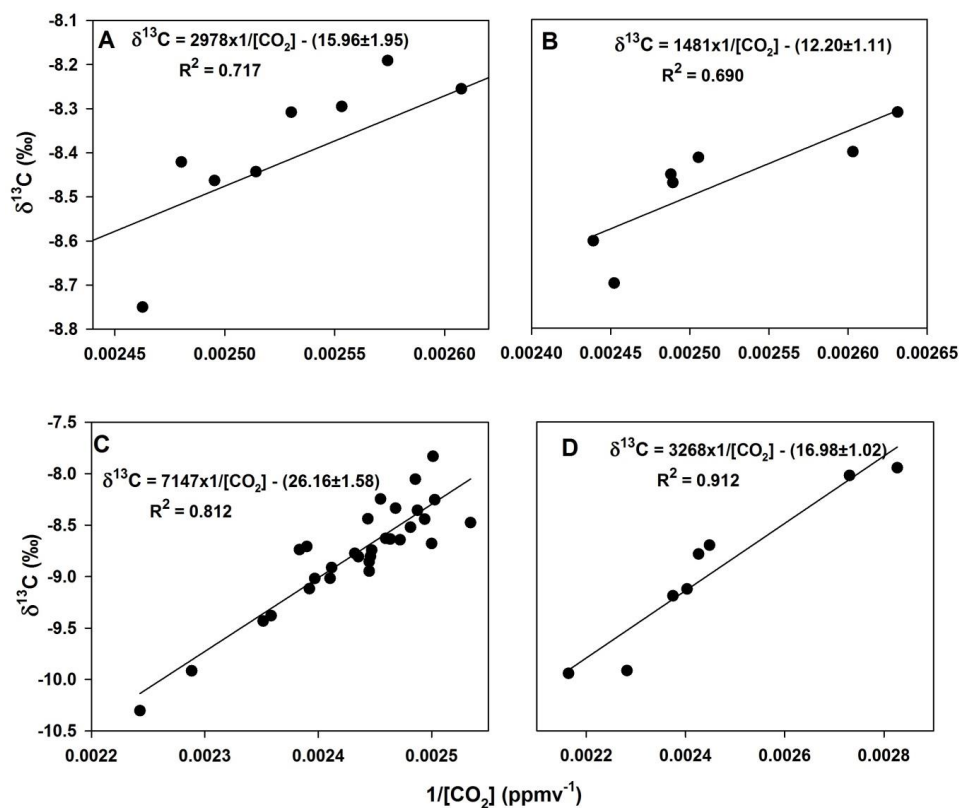
874 Figure 4. Correlation between the observed and thermodynamic equilibrium  $\Delta_{47}$  values for  
 875 greenhouse  $\text{CO}_2$  samples collected when (A) photosynthesis is weak and respiration is strong  
 876 and (B) photosynthesis is strong and respiration is weak.

877

878

879





880

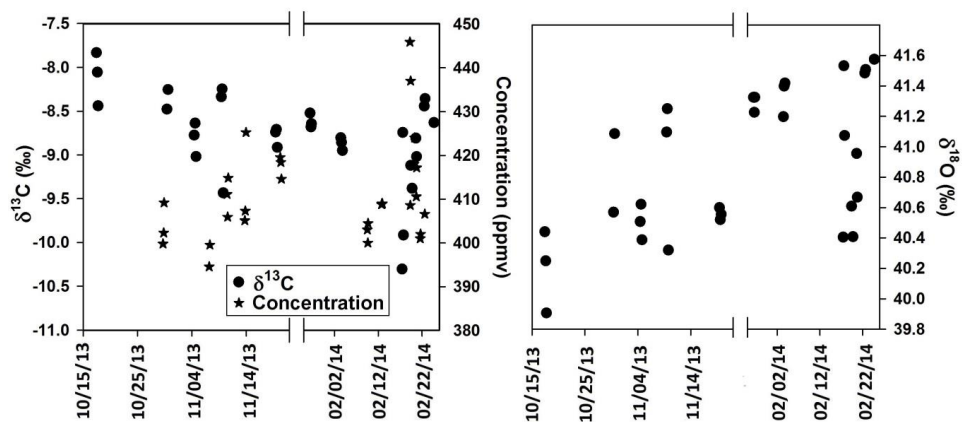
881 Figure 5. Carbon Keeling plots for atmospheric CO<sub>2</sub> collected at (A) South China Sea (B)

882 Keelung and Fuguei Cape, (C) sub-urban station, Academia Sinica Campus, and (D)

883 grassland, National Taiwan University. For more details about the sites, see the texts and

884 Figure 1.

885

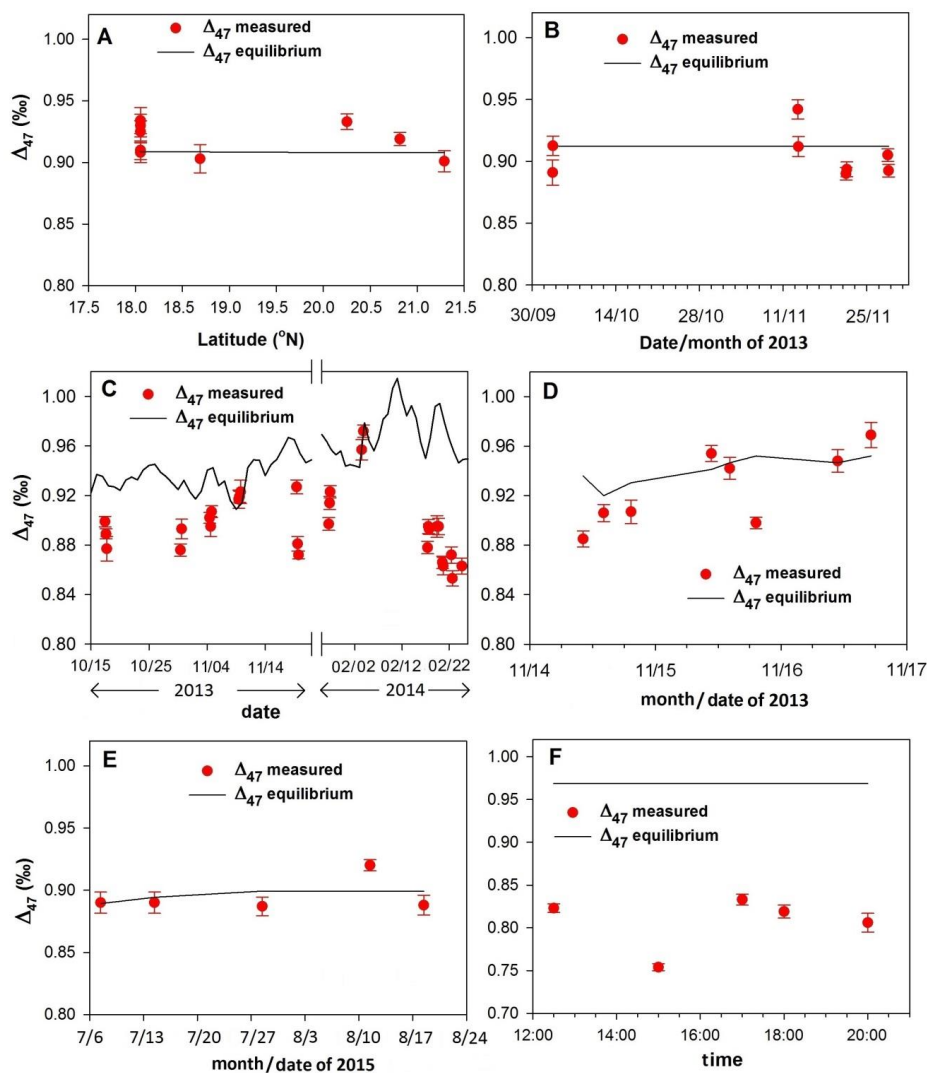


886

887 Figure 6. Time series of (A) concentration and stable carbon and (B) stable oxygen isotopes

888 for CO<sub>2</sub> collected at Academia Sinica Campus.

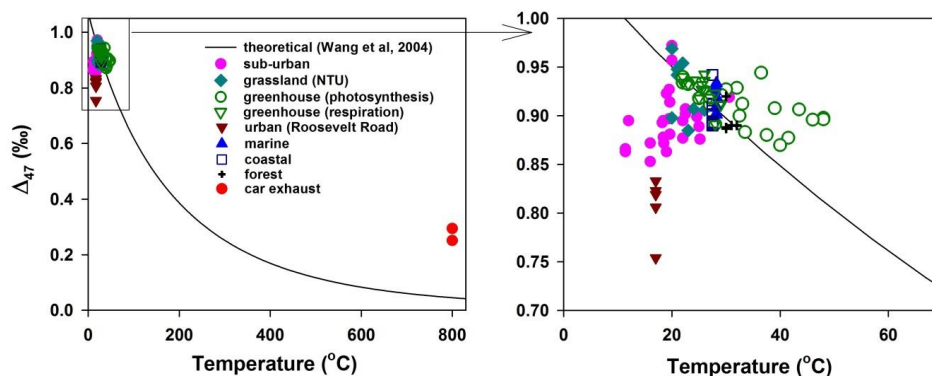
889



890  
 891 Figure 7.  $\Delta_{47}$  values in the near surface atmospheric  $\text{CO}_2$  from (A) South China Sea, (B)  
 892 coastal stations (Keelung and Fuguei Cape), (C) sub-urban station (Academia Sinica  
 893 campus), (D) grassland in the National Taiwan University campus, (E) forest site near the  
 894 Academia Sinica Campus and (F) urban site (Roosevelt Road). The error bars are the 1  
 895 standard errors associated with the measurements. Lines show  $\Delta_{47}$  values for the  $\text{CO}_2$  in  
 896 thermodynamic equilibrium at ambient temperatures.



897



898

899

900 Figure 8. A summary of  $\Delta_{47}$  values in near surface air  $\text{CO}_2$  obtained at different environments  
901 and compared with the thermodynamic equilibrium values. Combustion temperature for car  
902 exhausts is assumed to be 800 °C (minimum value). Greenhouse  $\text{CO}_2$  are divided into two  
903 categories: photosynthesis dominated (green open circle) and respiration dominated (green  
904 open triangle).

905

906

907

908

909

910

911

912

913

914

915

916



Table 1. Reproducibility and precision of measurements for stable isotopes including  $\Delta_{47}$  for IAEA NBS-19.

Sl. No.	$\delta^{13}\text{C}$ (‰) (VPDB)	$\delta^{18}\text{O}$ (‰) (VPDB $\text{CO}_2$ )	$\delta^{\text{H}}$ (‰)	Std. Err.	$\Delta_{47}$ (‰)	Std. Err.
1	2.02	-2.21	35.22	0.01	0.382	0.010
2	2.02	-2.11	35.54	0.02	0.394	0.012
3	2.02	-2.19	35.28	0.01	0.416	0.010
4	2.01	-2.28	35.15	0.01	0.408	0.011
5	2.00	-2.27	35.24	0.02	0.388	0.016
6	2.00	-2.16	35.27	0.02	0.370	0.013
7	2.02	-2.27	35.21	0.01	0.398	0.009
8	2.02	-2.20	36.48	0.01	0.363	0.008
9	2.01	-2.20	36.56	0.02	0.392	0.006
10	2.01	-2.15	36.46	0.01	0.399	0.012
11	2.01	-2.20	36.57	0.01	0.393	0.010
12	2.02	-2.21	36.32	0.01	0.387	0.009
13	2.01	-2.18	36.43	0.01	0.368	0.014
14	2.01	-2.16	35.81	0.01	0.379	0.010
15	2.00	-2.18	35.76	0.01	0.387	0.006
Average	2.01	-2.20	35.82		0.388	
Std. Dev.	0.01	0.05	0.58		0.014	



922 Table 2. Diurnal variation of  $\delta^{13}\text{C}$  and  $\delta^{18}\text{O}$  and clumped isotopes ( $\Delta_{47}$ ) for greenhouse  $\text{CO}_2$ . Temperatures estimated using  $\Delta_{47}$  values and actual air  
 923 temperatures inside the greenhouse at the time of sampling are also presented.  
 924

Date	Time	Conc. (ppmv)	$\delta^{13}\text{C}$ (‰) (VPDB)	$\delta^{18}\text{O}$ (‰) (VSMOW)	$\delta^{47}$ (‰)	Std. err.	$\Delta_{47}$ (‰) (ARF)	Std. err.	Estimated temp. (°C)	Air temp. (°C)
7/28/2015	4:50	481	-11.60	39.61	6.99	0.02	0.927	0.016	24	25.5
	6:00	462	-10.90	39.92	8.16	0.02	0.936	0.018	21	26
	7:06	435	-9.80	40.54	9.71	0.02	0.911	0.017	28	29
	8:10	428	-9.60	40.92	10.38	0.02	0.883	0.014	33	33.5
	9:15	416	-9.06	41.36	11.30	0.01	0.908	0.011	24	39
	10:15	422	-9.55	40.82	NA	NA	NA	NA	NA	NA
7/31/2015	12:40	407	-8.77	41.58	11.75	0.01	0.898	0.010	27	48
	5:00	522	-12.72	38.66	5.10	0.01	0.926	0.015	24	26
	6:00	512	-12.37	38.95	5.94	0.01	0.926	0.014	25	26
	7:00	451	-10.08	40.36	9.39	0.02	0.923	0.011	25	28
	8:15	405	-8.82	40.98	11.25	0.02	0.912	0.020	28	33
	9:10	412	-9.12	41.07	11.26	0.02	0.880	0.020	34	37.5
	10:00	414	-9.35	40.83	11.52	0.01	0.906	0.010	23	43.5
	11:20	411	-9.26	40.99	11.12	0.02	0.896	0.025	31	48
	15:00	432	-9.90	40.36	9.55	0.02	0.877	0.015	34	41.5
	17:25	423	-9.22	41.07	12.48	0.02	0.929	0.013	25	32
8/4/2015	21:30	462	-10.92	39.99	7.90	0.01	0.911	0.012	28	27
	4:50	465	-11.03	40.37	8.41	0.01	0.936	0.012	23	24
	5:50	455	-10.82	40.26	NA	NA	NA	NA	NA	NA
	6:28	448	-10.27	41.00	10.01	0.02	0.931	0.017	24	25.5
	6:50	439	-9.90	41.32	10.10	0.02	0.942	0.009	22	26



	7:15	420	-9.34	41.22	11.05	0.01	0.914	0.013	28	28.5
	7:40	419	-9.18	41.22	11.05	0.01	0.927	0.011	25	30
	8:10	405	-8.55	41.56	12.79	0.02	0.900	0.015	31	32.5
	9:45	427	-9.75	40.73	10.81	0.02	0.870	0.023	36	40
	14:00	414	-9.20	41.01	11.02	0.01	0.896	0.011	31	46
	16:15	414	-9.09	41.11	11.11	0.01	0.944	0.014	22	36.5
	19:15	413	-9.01	41.38	13.28	0.01	0.921	0.010	26	29.2
	22:30	450	-10.58	40.61	9.34	0.02	0.924	0.022	25	26.5
	5:45	418	-9.30	40.87	10.80	0.01	0.934	0.013	23	22
	7:00	413	-9.08	41.18	10.95	0.02	0.940	0.021	22	22
	10:00	390	-7.78	41.66	13.00	0.02	0.918	0.014	26	25
	11:50	388	-7.84	41.71	15.25	0.01	0.919	0.010	26	27
	14:30	382	-7.82	42.24	14.27	0.02	0.891	0.017	31	28
	20:10	418	-9.17	40.61	10.85	0.02	0.933	0.017	23	23
	10/12/2015									

Table 3. Stable carbon and oxygen isotopic composition and clumped isotopes ( $\Delta_{47}$ ) for car exhaust  $\text{CO}_2$ . Temperatures estimated using  $\Delta_{47}$  values and lowest possible combustion temperatures are given.

Car model	Conc. (ppm)	$\delta^{13}\text{C}$ (‰) (VPDB)	$\delta^{18}\text{O}$ (‰) (VSMOW)	$\delta^{47}$ (‰)	Std. err.	$\Delta_{47}$ (‰) (ARF)	Std. err.	Estimated temp. (°C)	Combustion temp. (°C)
Mazda 3000cc TRIBUTE	39400	-27.73	25.43	-22.20	0.01	0.251	0.013	300	800
Mitsubishi 2400cc New Outlander	39300	-27.67	25.27	-23.08	0.02	0.294	0.007	265	800
Average $\pm 1\sigma$	39350 $\pm$ 50	-27.70 $\pm$ 0.03	25.35 $\pm$ 0.07	-22.64 $\pm$ 0.44		0.273 $\pm$ 0.021		283 $\pm$ 18	



933  
 934  
 935  
 936  
 937

Table 4. Stable isotopic composition including  $\Delta_{47}$  for air CO<sub>2</sub> collected over South China Sea and two coastal stations (see Figure 1 for sampling locations). Temperatures estimated using  $\Delta_{47}$  values and the sea surface temperatures at the time of samplings are also presented.

Marine air CO <sub>2</sub>										
South China Sea										
Date time	Conc. (ppm)	$\delta^{13}\text{C}$ (‰) (VPDB)	$\delta^{18}\text{O}$ (‰) (VSMOW)	$\delta^{47}$ (‰)	Std. err.	$\Delta_{47}$ (‰) (ARF)	Std. err.	Estimated temp. (°C)	Sea surface temp. (°C)	
10/15/2013 8:15 (A)*	403	-8.42	40.85	28.752	0.016	0.901	0.017	30	28.3	
10/15/2013 13:15 (B)	400	-8.46	40.80	28.441	0.012	0.919	0.011	26	28.3	
10/15/2013 18:00 (C)	406	-8.75	40.54	28.133	0.013	0.933	0.013	24	28.3	
10/16/2013 7:00 (D)	391	-8.76	40.53	27.916	0.024	0.903	0.023	29	28.2	
10/16/2013 12:05 (E)	397	-8.44	40.86	28.535	0.015	0.910	0.015	28	28.2	
10/16/2013 14:00 (E)	391	-8.30	40.96	28.922	0.021	0.934	0.021	23	28.2	
10/16/2013 17:20 (E)	395	-8.31	41.02	28.944	0.017	0.908	0.016	29	28.1	
10/16/2013 20:20 (E)	388	-8.19	40.52	28.909	0.018	0.930	0.018	24	28.1	
10/17/2013 8:40 (E)	383	-8.26	40.41	28.194	0.018	0.925	0.018	25	28.1	
Average $\pm 1\sigma$	395 $\pm$ 7	-8.43 $\pm$ 0.19	40.72 $\pm$ 0.20	28.52 $\pm$ 0.36		0.918 $\pm$ 0.012		27 $\pm$ 2	28.2 $\pm$ 0.1	
Keelung										
10/03/2013 11:30	380	-8.31	40.31	28.053	0.020	0.896	0.021	31	27.5	
10/03/2013 12:30	384	-8.40	40.92	29.089	0.017	0.917	0.016	27	27.5	





<b>Fuguei Cape</b>												
11/13/2013 11:00	401	-8.45	40.62	29.645	0.015	0.946	0.016	21	27.5			
11/21/2013 12:30		-8.47	40.78	29.866	0.017	0.890	0.010	32	27.5			
11/28/2013 12:00	410	-8.60	40.21	28.992	0.011	0.908	0.010	28	27.5			
Average ± 1σ	394±12	-8.45±0.09	40.57±0.26	29.12±0.63		0.911±0.020		28±4	27.5			
<b>Fuguei Cape</b>												
11/13/2013 13:30	401	-8.47	40.76	29.56	0.02	0.916	0.016	27	27.5			
11/21/2013 15:30	399	-8.41	40.89	29.37	0.01	0.880	0.012	34	27.5			
11/28/2013 15:00	407	-8.70	41.16	30.11	0.01	0.886	0.010	33	27.5			
Average ± 1σ	402±3	-8.53±0.12	40.94±0.16	29.68±0.29		0.894±0.015		31±3	27.5			

\*Sampling Stations (see Figure 1 for locations in South China Sea)

Table 5. Stable isotopic composition including clumped isotopes ( $\Delta_{47}$ ) for air CO<sub>2</sub> collected in urban and sub-urban stations, grassland, forest and high mountain environments. Temperatures estimated using  $\Delta_{47}$  values and air temperatures are also presented.

<b>Urban CO<sub>2</sub>: Roosevelt Road, Taipei City</b>										
Date	Time	Conc. (ppm)	$\delta^{13}\text{C}$ (‰) (VPDB)	$\delta^{18}\text{O}$ (‰) (VSMOW)	$\delta^{47}$ (‰)	Std. err.	$\Delta_{47}$ (‰) (ARF)	Std. err.	Estimated temp. (°C)	Air temp. (°C)
12/30/2015	12:30	510	-10.41	40.00	25.26	0.014	0.823	0.010	46	20
	15:00	478	-11.50	38.49	22.63	0.012	0.754	0.008	62	19.5
	17:00	461	-9.69	40.70	26.74	0.017	0.833	0.013	44	17
	18:00	594	-12.30	38.14	21.56	0.014	0.819	0.015	47	16
	20:00	457	-11.34	39.24	23.61	0.022	0.806	0.022	50	15
Average±1σ		500±50	-11.05±0.90	39.31±0.94	23.96±1.84		0.807±0.028		50±6	17±2

938  
 939  
 940  
 941  
 942  
 943  
 944  
 945



Sub-urban air CO <sub>2</sub>										
Academia Sinica Campus										
Date time	Conc. (ppm)	$\delta^{13}\text{C}$ (‰) (VPDB)	$\delta^{18}\text{O}$ (‰) (VSMOW)	$\delta^{47}$ (‰)	Std. err.	$\Delta_{47}$ (‰) (ARF)	Std. err.	Estimated temp. (°C)	Air temp (°C)	
10/17/2013 10:00	400	-7.83	40.44	28.47	0.015	0.899	0.008	30	25	
10/17/2013 14:30	402	-8.05	40.25	28.07	0.017	0.889	0.008	32	25	
10/17/2013 17:20	409	-8.44	39.90	27.26	0.019	0.877	0.020	34	22	
10/30/2013 10:00	395	-8.48	40.57	28.47	0.012	0.876	0.010	35	25.2	
10/30/2013 14:30	400	-8.25	41.08	29.03	0.016	0.893	0.016	31	27.4	
11/04/2013 10:30	411	-8.78	40.51	28.67	0.011	0.902	0.009	29	22.5	
11/04/2013 14:30	406	-8.64	40.62	28.97	0.017	0.895	0.016	31	22	
11/04/2013 18:30	415	-9.02	40.38	28.33	0.013	0.907	0.009	28	22.5	
11/09/2013 10:30	405	-8.34	41.09	29.79	0.019	0.917	0.015	27	28.5	
11/09/2013 14:00	407	-8.25	41.25	30.63	0.015	0.919	0.009	26	30.6	
11/09/2013 18:30	425	-9.43	40.32	27.49	0.020	0.923	0.019	25	28	
11/19/2013 10:00	419	-8.74	40.60	29.27	0.012	0.927	0.011	25	19.5	
11/19/2013 14:00	418	-8.71	40.52	29.59	0.019	0.881	0.012	33	19.6	
11/19/2013 18:00	414	-8.91	40.56	28.58	0.012	0.872	0.006	35	18.5	
01/27/2014 10:30	403	-8.52	41.32	30.13	0.008	0.897	0.010	30	19.2	
01/27/2014 15:20	400	-8.68	41.23	30.03	0.011	0.914	0.010	27	19.6	
01/27/2014 18:00	404	-8.64	41.32	29.29	0.017	0.923	0.010	25	18.5	
02/03/2014 11:00	408	-8.80	41.20	29.67	0.015	0.957	0.017	19	24.5	
02/03/2014 14:30	409	-8.86	41.39	NA		NA				
02/03/2014 19:30	409	-8.95	41.41	30.57	0.011	0.972	0.010	16	19.3	



02/17/2014 10:30	445	-10.30	40.40	27.60	0.016	0.878	0.010	34	22.4	
02/17/2014 14:30	408	-8.74	41.53	30.58	0.014	0.895	0.011	31	25	
02/17/2014 18:30	437	-9.92	41.07	28.49	0.012	0.893	0.008	31	22	
02/19/2014 10:00	418	-9.12	40.61	29.12	0.020	0.895	0.018	31	13.3	
02/19/2014 18:00	424	-9.38	40.40	28.49	0.020	0.895	0.013	31	12.4	
02/20/2014 14:30	410	-8.81	40.96	29.68	0.023	0.866	0.010	37	12.9	
02/20/2014 18:00	417	-9.02	40.66	29.59	0.018	0.863	0.014	37	12.5	
02/22/2014 12:15	401	-8.44	41.49	30.63	0.013	0.872	0.013	35	17.5	
02/22/2014 17:00	402	-8.36	41.51	30.63	0.013	0.853	0.012	40	17.1	
02/24/2014 17:30	406	-8.63	41.57	30.70	0.014	0.863	0.013	37	22	
Average ± 1σ	411±11	-8.78±0.50	40.87±0.46	29.23±1.00		0.897±0.027		30±5	21±5	
<b>Grassland: NTU Campus</b>										
11/14/2013 10:10	353	-7.95	40.96	30.18	0.02	0.885	0.013	33	23	
11/14/2013 14:05	366	-8.02	41.31	30.79	0.01	0.906	0.014	29	26	
11/14/2013 19:20	462	-9.94	38.33	25.64	0.02	0.907	0.019	29	24	
11/15/2013 10:40	416	-9.12	39.42	29.51	0.01	0.954	0.013	20	22	
11/15/2013 14:10	421	-9.19	39.36	29.78	0.02	0.942	0.018	22	21	
11/15/2013 19:12	438	-9.92	38.28	28.08	0.04	0.989	0.009	13	20	
11/16/2013 10:50	412	-8.78	40.03	28.54	0.02	0.948	0.018	21	21	
11/16/2013 17:10	408	-8.70	40.26	26.06	0.02	0.969	0.021	17	20	
Average ± 1σ	409±33	-8.95±0.70	39.74±1.00	28.57±1.77		0.937±0.030		23±6	22±2	
<b>Forest site near Academia Sinica Campus</b>										
07/07/2015 10:30	411	-9.07	41.43	11.54	0.01	0.890	0.017	32	32	
07/14/2015 10:30	458	-10.43	39.74	9.01	0.02	0.890	0.017	32	31	
07/28/2015 10:40	441	-9.99	40.86	10.07	0.02	0.887	0.015	32	30	
08/11/2015 10:40	448	-10.46	40.09	9.50	0.01	0.920	0.009	26	30	



08/18/2015 10:30	433	-9.99	39.80	8.99	0.02	0.888	0.016	32	30
Average ± 1σ	438±16	-9.99 ±0.50	40.39±0.66	9.82±0.94		0.895±0.012		31±2	31±1
<b>High mountain: Hehuan</b>									
10/09/2013 13:20	364	-8.21	40.89	28.79	0.02	0.895	0.016	31	10
10/09/2013 17:00	NA	-8.25	40.28	28.41	0.01	0.914	0.014	27	10
Average ± 1σ	364	-8.23 ±0.02	40.59±0.30	28.60±0.19		0.904±0.009		30±2	10